
Picturing thermal niches and biomass of hydrothermal vent species

Husson Bérengère ^{1,*}, Sarradin Pierre-Marie ¹, Zeppilli Daniela ¹, Sarrazin Jozée ¹

¹ IFREMER, Centre de Bretagne, REM/EEP, Laboratoire Environnement Profond, Institut Carnot EDROME, F-29280 Plouzané, France

* Corresponding author : Bérengère Husson, Tel.: +33(0)298224040 ;
email address : berengere.husson@ifremer.fr

Abstract :

In community ecology, niche analysis is a classic tool for investigating species' distribution and dynamics. Components of a species' niche include biotic and abiotic factors. In the hydrothermal vent ecosystem, although composition and temporal variation have been investigated since these deep-sea habitats were discovered nearly 40 years ago, the roles and the factors behind the success of the dominant species of these ecosystems have yet to be fully elucidated. In the Lucky Strike vent field on the Mid Atlantic Ridge (MAR), the dominant species is the mussel *Bathymodiolus azoricus*. Data on this species and its associated community were collected during four oceanographic cruises on the Eiffel Tower edifice and integrated in a novel statistical framework for niche analysis. We assessed the thermal range, density, biomass and niche similarities of *B. azoricus* and its associated fauna.

Habitat similarities grouped mussels into three size categories: mussels with lengths ranging from 0.5 to 1.5 cm, from 1.5 to 6 cm, and mussels longer than 6 cm. These size categories were consistent with those found in previous studies based on video imagery. The three size categories featured different associated fauna. The thermal range of mussels was shown to change with organism size, with intermediate sizes having a broader thermal niche than small or large mussels. Temperature maxima seem to drive their distribution along the mixing gradient between warm hydrothermal fluids and cold seawater. *B. azoricus* constitutes nearly 90% of the biomass (in g dry weight /m²) of the ecosystem. Mean individual weights were calculated for 39 of the 79 known taxa on Eiffel Tower and thermal ranges were obtained for all the inventoried species of this edifice. The analysis showed that temperature is a suitable variable to describe density variations among samples for 71 taxa. However, thermal conditions do not suffice to explain biomass variability. Our results provide valuable insight into mussel ecology, biotic interactions and the role of *B. azoricus* in the community.

Keywords : *Bathymodiolus azoricus*, OMI, Habitat, Niche, Mid-Atlantic ridge, Lucky strike

1 Introduction

The scientific concepts of the limits of life in the deep ocean were pushed back in 1977 with the discovery of organisms proliferating around hydrothermal vents (Corliss et al., 1979). Since then, these communities and their physico-chemical habitats have been extensively studied worldwide: in the Pacific (e.g. Kim and Hammerstrom, 2012; Lutz et al., 2008; Sarrazin and Juniper, 1999; Sen et al., 2013; Urcuyo et al., 2003), Atlantic (e.g. Copley et al., 2007, 1997; Fabri et al., 2011; Sarrazin et al., 2015; Van Dover and Doerries, 2005), and Indian (e.g. Van Dover et al., 2001) oceans. Vent communities are often dominated by invertebrates living in association with symbionts (Léveillé et al., 2005) such as siboglinid tubeworms in the Pacific and bathymodiolin mussels or bresiliid shrimp in the Mid-Atlantic Ridge (MAR), which aggregate in patches (e.g. Tsurumi and Tunnicliffe, 2001). However, much is still unknown about what determines the success of these species and the factors behind the distribution of their associated communities.

The ecological niche is a key concept in understanding species distribution. It refers to a fundamental concept in community ecology that was developed by Grinnell (1917) and Elton (1927). The Grinnellian niche deals with the impact of the geographical habitat, including its biotic and abiotic components, on the distribution of a species at a location, whereas the Eltonian niche focuses more on biotic aspects, such as the trophic food web and interspecific competition. Later, the ecological fundamental niche of a species was defined by Hutchinson (1957) as the hypervolume defined by abiotic and biotic conditions and resource ranges in which a species can survive. Niche breadth, also called niche width (see e.g. Colwell and Futuyma, 1971), is thus interpreted as the range of abiotic conditions that a species can cope with; the interspecific degree of niche overlap provides insights on potential biotic competitions. The realised niche is the combined result of environmental conditions and

biotic pressure. More recently, Chase and Leibold (2003) enriched the concept by including the impact of a species on the ecological factors of its niche in the definition of a niche.

Biotic and abiotic components of hydrothermal vent species niches have often been studied separately. Along the dilution gradient between seawater and hydrothermal fluids, highly variable physico-chemical conditions strongly structure species assemblages (Gollner et al., 2010a; Luther et al., 2001; Marsh et al., 2012; Podowski et al., 2010; Sarrazin et al., 1999). Survival capacities of vent species in these warm, hypoxic and toxic environments have been the focus of several studies (e.g. Bates et al., 2010; Shillito et al., 2006). Given that temperature is linked to the dilution of the hot hydrothermal fluid in the cold ambient seawater (Le Bris et al., 2006), warmer environments are generally also more toxic. Behavioural strategies and metabolic mechanisms involved in the tolerance to toxic components have been studied in hydrothermal species dealing with constraining conditions (e.g. Company et al., 2004; McMullin et al., 2000).

Biotic interactions are mainly investigated through trophic networks, estimated using stable isotopes and fatty acids (e.g. Colaço et al., 2002; De Busserolles et al., 2009; Portail et al., 2015). Fewer studies have simultaneously estimated the biomass and the link between density distributions and food-web structure (Bergquist et al., 2007). Due to the restrictions of working in an isolated and extreme environment, competition, territoriality and predatory behaviour are more recent topics in deep-sea research which require setting up manipulative field experiments (Levesque et al., 2003; Micheli et al., 2002) or analysing imagery (Grelon et al., 2006; Matabos et al., 2015; Podowski et al., 2009; Sen et al., 2013). Species assemblage distribution and composition also rely on the succession of species that occurs during the colonising processes after disturbance (e.g. Shank et al. 1998, Mullineaux et al. 2010, Gaudron et al. 2012, Sen et al. 2014, Gollner et al. 2015a). Observed successional patterns

include both facilitation and inhibition phenomena (e.g. Mullineaux et al. , 2012, 2003; Sarrazin et al., 2002).

On the MAR, two northern vent fields, Menez Gwen and Lucky Strike, are dominated by the bathymodiolin mussel *Bathymodiolus azoricus* (Desbruyères et al., 2001). The mussel was described by (Cuvelier et al., 2011a) as the climax community on the Eiffel Tower vent edifice in Lucky Strike vent field. The factors that determine its success and that of its associated community are still poorly understood. The aim of this study was to further assess the success and role of *B. azoricus*, through the analysis of its niche and those of its associated community. Using a novel statistical framework, we addressed the following questions: (i) what is the thermal range in which *B. azoricus* and its associated species occur? (ii) what are the biotic descriptors (densities, biomasses and niche similarities) of the whole community? We used both density and biomass data to gain insight on the role of *B. azoricus* in the community. All data were collected on the well-studied Eiffel Tower edifice located in the Lucky Strike vent field.

2 Materials and Methods

2.1 Study site

Discovered in 1992 during the FAZAR expedition, Lucky Strike (LS) is a basalt-hosted vent field (Langmuir et al., 1997) situated in the Azores Triple Junction on the MAR (37°17.29'N, 32°16.45'W) at a mean depth 1700 m (Desbruyères et al., 2001). More than 20 sulphide edifices are distributed around a large central lava lake (Ondréas et al., 2009) with a magmatic chamber located at 3 km depth (Singh et al., 2006). The hydrothermal fluids of LS are strongly controlled by geological settings in four areas (north-western, north-eastern,

south-western and south-eastern areas), with the source of the south-eastern region being different from the three others (Barreyre et al., 2012). The Eiffel Tower edifice is the most studied vent edifice of this south-eastern region (Figure 1A and B). This 11 m high sulphide edifice has been thoroughly studied for more than 20 years. The edifice consists of a massive sulphide deposit and an underlying surrounding periphery that extends out to about 20 m (Cuvelier et al., 2009). Hydrothermal activity occurs through black smokers, flanges or diffusion zones, while the eastern peripheral zone shows no activity (Cuvelier et al., 2009). The temperatures of the focused emissions can reach 324°C, with pH values ranging from 3.4 to 5.6. The fluids are generally richer in sulphide than in methane (Charlou et al., 2000).

Faunal colonisation of vent ecosystems occurs only toward the end of the dilution gradient. Out of the six assemblages characterised by Cuvelier et al. (2009), five are visually dominated by mussels, differing in size and in the presence or absence of microbial mats, that colonise a narrow range of low temperature habitats. Indeed, mean temperatures range from 4.8°C to 8.8°C (Sarrazin et al., 2015) in the mussel assemblages. The sixth assemblage defined by Cuvelier et al. (2009) is composed of shrimp, mainly *Mirocaris fortunata* that inhabit warmer habitats, with temperature up to an average of 9.5°C (Cuvelier et al., 2011b). The diversity varies strongly along the fluid mixing gradient, with higher densities and species richness observed in low temperature habitats (Sarrazin et al., 2015)

2.2 Sample collection

The data used in this study come from four different cruises carried out on the Eiffel Tower edifice with the ROV *Victor6000* between 2005 and 2014 (Table 1). Two of these cruises, EXOMAR and MOMARETO, provided faunal inventories whose data were used here for community biomass and niche analyses. The third cruise, MoMARSAT 11, allowed the

collection and computation of meiofaunal biomass. Finally, the fourth cruise, MoMARSAT 14, produced additional biomass data for macrofauna (Table 1).

During EXOMAR, five neighbouring assemblages of small mussels and their associated communities were sampled (Table 2) while during MOMARETO, 12 distinct mussel assemblages were exhaustively sampled (Table 2, see Sarrazin et al. 2015 for major results and sampling details). Both cruises used the same sampling protocol: (i) discrete temperature measurements prior to sampling using the ROV temperature probe (EXOMAR) or an autonomous NKE (MOMARETO) temperature probe at several points in the assemblage, during at least 2 minutes; (ii) faunal sampling using the ROV suction sampler and arm grab, as described in Cuvelier et al. (2012); (iii) on board, sample sieving through a 63 μm mesh and sample preservation. Taxa coming from both cruises have sometimes been identified at different taxonomic resolutions. In these cases, higher taxa names were used and included in all analyses. To compare samples using the same set of environmental factors, only temperature data ($^{\circ}\text{C}$) were used in this study. Temperature was shown to be a good proxy for the chemical habitats, especially on a known hydrothermal site (Le Bris et al., 2006). During MoMARSAT 11, size measurements were used to evaluate meiofaunal biomass (Table 1 see Zeppilli et al. (2015) for major results and sampling details).

For the three cruises during which mussel assemblages were sampled (Table 1) all mussel shells longer than 5 mm were measured (Table 2). Some shells were crushed and unmeasurable, but were more or less of the same size range as those measured in the same sample. Crushed shells in a given sample did not amount to more than 17.1% of the total number of mussels collected, except for one MOMARETO sample (06_6, see Table 2), for which crushed shells constituted 49.2% of the total number of mussels. Mussels with shells

smaller than 5 mm were considered juveniles. Sampled surfaces were estimated in triplicate using imagery analysis with ImageJ© software (rsb.info.nih.gov/ij/).

2.3 Biomass experiments

Length-weight relationships were modelled for three taxa: *B. azoricus*, *M. fortunata* and at least three unidentified polynoid polychaete taxa (Table 3). All other mean individual weights were obtained by pooling individuals together to measure their biomass or were based on published literature. Total wet weight (flesh and shell), flesh wet weight, dry weight, ash weight, and ash-free dry weight were measured individually on a total of 791 *B. azoricus* from 3 cruises (Table 1). Dry weights were measured after at least 24 h at 60°C and ash weights were measured after at least 12 h at 550°C. These data were used to model length-weight relationships following the standard equation:

$$(1) W = aL^b$$

where W is the calculated weight (g) and L the (straight) length of the body (or the shell, for *B. azoricus*), measured with a calliper, in mm. Regression coefficients a and b were computed using log-normal regression. Residual normality and homoscedasticity were validated visually. The analysis of variance of the model revealed a strong cruise effect, with the EXOMAR cruise having the strongest effect, and normality of residuals was not validated. Therefore, the EXOMAR data were removed and a second model using the 334 mussels from the MOMARETO and MoMARSAT 14 cruises only was validated, and used in the rest of the analysis (Table 3). Biomass of all other measured mussels was calculated using the second, validated model. Juvenile mussel biomass was estimated by applying the model for a length of 4.9 mm and multiplying the result by juvenile density in each sample. Although the length-weight relationship was based on mussels with shell lengths at least 5 mm, the value of 4.9 was chosen so that the extrapolation of the juvenile weight would be as close to the limits of the relationship as possible. Therefore, juvenile biomass was likely over-

estimated. Similarly, the length-weight relationships were modelled on 259 polynoids (mainly *Branchiopolynoe seepensis*) and 90 *M. fortunata* shrimp from MoMARSAT cruises (Table 3). When the number of specimens was not sufficient to model length-weight relationships, individuals were pooled to obtain mean individual dry weights. If the number of individuals was not sufficient, mean individual dry weights were taken from the literature on deep-sea fauna, sometimes from a different ecosystem (e.g., Tanaidacea, whose weight was calculated from abyssal plains, and may thus not have the same size as sampled individuals). Conversion coefficients were used to obtain species dry weights (Ricciardi and Bourget, 1998) when needed.

Biomass were calculated for copepods using the volumetric equation by Warwick and Price (1979):

$$(2) V = C \cdot L \cdot w^2$$

where V is the volume in nL, L the length and w width of the body in mm, and C is a dimensionless shape factor. The shape factor used is from Warwick and Gee (1984). For nematodes, the formula by Andrassy (1956) was preferred:

$$(3) V = L \times w^2 \times 0.063 \times 10^{-5}$$

2.4 Data analysis

Our study is divided into two parts. The first part focuses on the biotic (biomass, density and niche similarities) and abiotic niche descriptors (thermal conditions) around *B. azoricus* (Analysis of mussel niche, Table 1). Niches of different mussel size classes are compared. The second part of the study assesses the same abiotic and biotic niche descriptors of the sampled community (Analysis of community niches, Table 1). Both parts use multivariate

analyses methods that require a principal component analysis (PCA) on environmental variables as a baseline. All analyses were performed in R 3.2.0 (R Core Team, 2015).

2.4.1 Thermal conditions and comparison of biomass and density among them

Four temperature descriptors were calculated for each sampling site: the mean (Mean.T), the minimum (Min.T), the maximum (Max.T) and the standard deviation (Std.T). Pearson's correlation was used to select non-redundant variables. Then, two PCAs were conducted on remaining temperature variables using the vegan package (Oksanen et al., 2015). The first PCA, hereafter referred as "PCA-mussel", was based on 21 sampling units from the EXOMAR, MOMARETO and MoMARSAT 14 cruises. The second PCA analysis, hereafter referred as "PCA-community", was conducted on 17 sites from the MOMARETO and EXOMAR cruises.

The centre of PCA-mussel and PCA-community represents the mean thermal conditions of the whole studied area, i.e. the average thermal conditions in mussel assemblages. A 2D kernel density, computed with the kde function in the ks package (Duong, 2015) and weighted by the square of the standardised relative density (or biomass) of the species at each sampling site, was applied on the plans defined by both PCAs. It maps, for a given species, areas of the PCA plot where high densities of sampling points with high species density or biomass are located, thus highlighting the "optimal" thermal niche of this species. Applied on PCA-mussel and PCA-community, it allowed to visualize and compare dry weight and density of respectively (i) *B. azoricus* and (ii) each sampled taxon among thermal conditions. Both PCA served as baseline for the rest of the analysis of mussel niche and the analysis of community niches respectively (Table 1). For PCA-community, the set of species was reduced to specimens for which both density and mean individual dry weights were available.

2.4.2 Building species niche

The niche of a set of species is studied using the outlier mean index (OMI) created by Dolédec et al. (2000), and computed using the “niche” function of R package ade4 (Dray et al., 2007). On a PCA of environmental parameters, sampling points are weighted by the species’ relative density or biomass. The centre of gravity of these weighted points is the species average position in the scatterplot defined by the PCA, i.e. the average environmental conditions in which a species thrives. The OMI, also called “marginality”, is a parameter that gives the squared distance between the species centre of gravity and the PCA centre. The higher this distance is, the more different the species niche thermal conditions are from the average conditions of the study (i.e. the centre of the PCA). A permutation test is used to check the significance of this index, indicating if species marginality is significantly higher than expected by chance. If significant, this test means that the species distribution is not independent of the environmental variables used in the PCA. Other output parameters of the OMI analysis are a measure of niche breadth: tolerance (Tol), which is the variance around the centroid, and the residual tolerance (RTol), which corresponds to the part of the variance that is not explained by the environmental variables used in the PCA, and thus indicates whether the chosen variables are suitable for the niche analysis. Marginality (OMI), tolerance (Tol) and residual tolerance (Rtol) constitute the total inertia of the niche and can be expressed as percentages of this inertia. At the same time, OMI analysis also identifies PCA environmental variables that best differentiate the niches of studied species. Graphic representation of the OMI analysis is a deformation of the PCA plot. This method is particularly efficient for describing species niches because, unlike other univariate or multivariate analyses, it does not make the assumption of a linear or unimodal response of faunal descriptors to environmental drivers.

OMI-mussel, based on PCA-mussel (Table 1) was conducted to describe the thermal niche of *B. azoricus* across different size classes. To do so, mussel lengths of all cruise data were included in 17 size categories, from <5 mm (juveniles) to >80 mm at 5 mm increments. Size categories can group mussels of similar weights; therefore there were no significant differences in any step of the analysis on biomass or density data, and only density results are shown. To highlight mussel size categories sharing the same thermal niche, outputs, i.e. (i) OMI, Tol and Rtol, along with (ii) the centre of gravity coordinates in the PCA plot, were used in a hierarchical clustering analysis, called HC-mussel, using the HCPC function in the R package FactoMineR (Husson et al., 2015). Thermal niche analyses of the community were performed using the OMI-community, based on the PCA-community. Only densities, which were available for each 79 taxon of the study, were used. To determine groups of taxa sharing similar thermal conditions, a hierarchical clustering analysis (HC-community) was performed.

2.4.3 Calculating niche overlap and testing similarity

Niche overlap between species was studied using Broennimann et al. (2012) methods. The 2D kernel density mapped on the PCA plot represents the niche of a species on a grid of size $R \times R$, where R is the number of rows and columns that divides the space (i.e. the resolution). Overlap between two niches is computed through the calculation of the metric D (Schoener, 1970):

$$D_{1,2} = 1 - 0.5 \sum_{ij} (p_{1ij} - p_{2ij})$$

where p_{1ij} and p_{2ij} are the values of each kernel density on the point of coordinates ij in the $R \times R$ grid. The calculated index, D , is comprised between 0 (no overlap) to 1 (complete overlap). A similarity test evaluates whether the observed D is greater than expected by chance. To compute the similarity between niche X and Y , niche Y is translated through the

PCA plot n times, n being the number of permutations chosen, and the overlap between X and the simulated niche Y is calculated. The same method is applied with a random X niche and a fixed Y niche. If the observed D is higher than 95% of all simulated values of D , then the niches are considered to be similar.

In the analyses of mussel niche (Table 1), a similarity test (SIM-mussel) was first conducted for each combination of the different size categories, with $n=100$ permutations each time. Similarly, in the analysis of the community niches (Table 1), similarity tests (SIM-community) were conducted on each pair of the 79 studied taxa, with $n=100$ permutations, to reveal taxon associations. Thermal ranges were extracted for each taxon.

3 Results

3.1 *Bathymodiolus azoricus* niche analysis

3.1.1 Thermal conditions in mussel assemblages

Mean temperature in mussel assemblages were comprised between 4.8 and 8.8°C, with minimum values of 3.7°C and maximum values of 14.2°C. Standard deviations varied from 0.1 to 2.7°C. As the standard deviations of temperature were strongly correlated with mean temperatures ($\text{corr}=0.92$), only Mean.T, Min.T and Max.T were used in PCA-mussel and PCA-community.

The PCA-mussel explained 96.7% of the variance, with 76.0% on the first axis (Figures 2A and B). All three variables were very well represented ($\sum \text{cos}^2=0.94, 0.99$ and 0.97 for Mean.T, Max.T, Min.T, respectively) and were strongly correlated with the first axis (95.8%, 73.9% and 90.4% for Mean.T, Max.T, Min.T, respectively). Max.T and Mean.T contributed strongly to the construction of the first axis (35.8 % and 40.2%, respectively). The second axis was only explained by Min.T ($\text{corr}=-0.67$, $\text{p.value}=0.0009$). All samples were very well

represented, with 05_4 (EXOMAR, Table 2) being the less well-represented sample with $\sum \cos^2=0.72$. Four samples (06_10, 06_8, 05_1 and 14_2) were more extreme and contributed strongly to the PCA plot (Table 2). PCA-mussel mapped two thermal zones with two subsections differentiated by minimal temperatures. On the PCA plot, the highest density of samples occurred on the right-hand side of the plot, close to the origins, indicating non-homogenous distribution along the thermal gradient (Figures 2A and B).

3.1.2 Mussel length-weight relationships

Mussels (n=334) were used for the calibration of the mussel length-weight relationships (Table 3). Flesh wet weight accounted for $40.03 \pm 10.08\%$ of total wet weight (i.e. with shell). Dry weight was about $14.31 \pm 4.05\%$ of flesh wet weight and $5.78 \pm 2.38\%$ of total wet weight. Ash weight accounted for $20.61 \pm 16.22\%$ of dry weight, $3.08 \pm 3.24\%$ of wet weight and $1.19 \pm 0.89\%$ of total wet weight. Finally, ash-free-dry-weight (AFDW) constituted $79.95 \pm 14.52\%$ of dry weight, $11.31 \pm 3.57\%$ of wet weight and $4.63 \pm 2.06\%$ of total wet weight. None of these values varied with mussel size, except for the ratio flesh wet weight-to-total wet weight, which increased slightly with size.

3.1.3 Mussel biomass along the gradient

In samples shown on PCA-mussel, mussels had an average density of 5977 ind./m^2 , with a range from 214 to $31\,630 \text{ ind./m}^2$. The highest densities were observed in the cooler habitats ($31\,630 \text{ ind./m}^2$ in 05_3, $15\,997 \text{ ind./m}^2$ in 14_1, Mean.T=6.1, Min.T=4.7, Max.T=9.15; Table 2) as shown by the weighted kernel density (Figure 2A). 80% of the highest densities (i.e. all samples comprised in the outermost 20% contour limit) were greater than 792 ind./m^2 . For this area, temperatures were greater than 4.4°C but less than the maximum of 9.2°C , with a mean of 5.4°C . Only four samples showed densities equivalent to or greater than 80% of

maximal weighed kernel density, with high variability, varying from 2 232 to 31 630 ind./m². Their temperatures ranged from 4.6 to 7.4°C, with a mean of 5.7°C (Figure 2A).

Estimated dry weights ranged from 74.3 to 3139.0 g/m², with a mean at 784.2 ± 724.9 g/m². In contrast to density data, total mussel biomass was higher on the left-hand side of the PCA plot, indicating higher dry weights in warmer habitats (3139 g/m² in sample 14_03, and 2187 g/m² in sample 14_2, Mean.T=6.8, Min.T=4.7, Max.T=14.2, Table 2, Figure 2B). However, the 20% and 40% contours extended to the right and also to the top left-hand part of the plot, showing relatively high biomass all along the thermal gradient. Samples located inside the 20% contour showed more than 214 ind./m² and 156.2 g dry weight/m², with a mean of 865.7 g dry weight/m². The thermal environment ranged from 4.4 to 14.1°C, with a mean of 5.6°C. The highest biomass, comprised in the 80% contour, had the same minimum biomass of 156.2 g dry weight/m², but a mean of 1121.9 g dry weight /m², indicating high variability in similar thermal environments (Figure 2B). Temperatures in this area were greater than 4.7°C but less than 9.2°C, with a mean of 6.2°C.

3.1.4 OMI analysis

As revealed by the OMI-mussel, each size category occupied a different thermal niche. This niche changed in overall position and in breadth with shell length (Figure 3A). Smaller size mussel niches are situated on the left-hand side of the niche plot, presenting low minimum, maximum, and mean temperatures, in contrast to larger size categories (Table 4). Mean position along the first axis (Figure 3B) moves toward warmer habitats with each increment in size, except for categories S11 and S16 (Table 4). Standard deviations widened between S1 to S12 before shrinking afterwards, indicating broader niches for mussels of intermediate size categories (between S8 and S14). From Figure 3A and B, each niche partially overlaps with neighbouring size categories, but smaller (S1 and S2) and larger (S15 and S16) niche categories are distinct. Mean position along the second axis did not vary with size, but

standard deviations increased for larger size classes, showing resistance to higher temperature maxima and minima (Figure 3A).

Residual tolerance ranged from 12.4 to 31.5% of total inertia; thus the variables used to describe the niches, i.e. mean, minimum and maximum temperatures at each sampling site explained 68.5 to 87.6% of niche distribution (Table 4). Marginality ranged from 1.3 to 70.1% of total inertia, with three different tendencies: (i) generally decreasing from 70.1% to 30.0% from S1 to S6, (ii) remaining below 10% from S7 to S12, and (iii) increasing again to 62.5% for S16. Intermediate size categories showed habitat preferences with a lower marginality (OMI), which means that the thermal conditions in which these mussels were found were similar to average conditions measured among all samples (the centre of the PCA). On the contrary, small and large size categories showed preferences for more marginal habitats. However, permutation tests gave significant p values only for juveniles, S15 and S16, indicating that only larger mussels and juveniles appear to select habitat based on temperature (or related factors). Tolerance varied from 8.6 to 74.1% of total inertia, with all tolerance above 65% being associated with size categories between S7 and S12 (35 to 65 mm of shell length).

3.1.5 Hierarchical clustering and similarity tests

OMI-mussel results and centroid coordinates were used in hierarchical clustering HC-mussel. The PCA built on these parameters by the clustering procedure explained 77.9% of the variability of which 45.8% by the first axis. All variables are well represented on the PCA plot, with $\sum \cos^2$ values comprised between 0.67 and 0.98. The clustering method that presented the lowest cophonetic correlation and highest Gower distance was the average method, and fusion levels favoured three clusters (Figure 4). Clustering was mainly driven by the centroid position along the first axis (centre of the ellipses), the OMI and the tolerance,

expressed as a percentage of inertia. (1) The first cluster included juveniles as well as size classes S1 to S6 and featured higher OMI, smaller ranges and first-axis coordinates that were more negative than average (Figure 4A). (2) The second cluster included size categories S7 to S13, and showed larger ranges and smaller OMI values than average (Figure 4B). (3) Finally, the third cluster included the higher size categories, from S14 to S16. It had higher OMI values, and also higher than average coordinates along the first and second axes (Figure 4C).

The similarity tests of SIM-mussel (Figure S.1) showed different results with three categories having a similar niches (juveniles, S1 and S2). The second group was composed of size S3 to S6, S7 being an intermediate niche for which overlap with all other niches was not significantly higher than expected by chance. The third group was composed of all other size categories (Figure S.1).

3.2 Niches analysis of the Eiffel Tower community

3.2.1 Thermal conditions

The PCA-community was very similar to the PCA-mussel (see 3.1.1). It explained 98.2% of the variability, with 80.4% on the first axis. All three variables were very well represented on the PCA- community ($\sum \text{Cos}^2 = 97.5, 99.9, 97.4$ for Mean.T, Min.T and Max.T, respectively). They were all significantly correlated with the first axis (96.3%, 93.9% and 77.7% for Mean.T, Max.T and Min.T, respectively), and all contributed almost equally to its construction, although Max.T and Mean.T tended to dominate (contribution = 36.5% and 38.4%, respectively, versus 25% for Min.T). On the other hand, as in PCA-mussel, the second axis was only explained by Min.T (corr=-0.63, p.value=0.007, contribution=74.2%). All sampling sites are very well represented, with the least represented sample being sample 05_4 with a $\sum \text{cos}^2$ of 0.56. The samples that contributed most strongly to the building of the PCA plot were the same as those in PCA-mussel, except 14_2 .

3.2.2 Species inventory

The inventory carried out during the EXOMAR cruise listed 41 meio- and macrofaunal taxa. During the MOMARETO cruise, a similar but more exhaustive sampling resulted in a list of 71 taxa, with 33 species in common with the EXOMAR inventory (Table 5). Only three species (*Paralepetopsis ferrugivora*, *Xylodiscula analoga* and *Alvinocaris markensis*), and other unidentified species from one family (Draconematidae, Nematoda), one order (Monhysterida, Nematoda) and one class (Alcyonaria, Cnidaria) were sampled during EXOMAR but not during MOMARETO (Table 5).

3.2.3 Mean community biomass

Mean individual dry weights were multiplied by density for each taxon for which the information was available. Average total density amounted to $169\,619 \pm 218\,472$ ind./m² for 940.1 ± 390.7 g dry weight/m². Nematodes and mussels dominated the overall density, accounting for respectively 61.0% and 25.6% of the total density, while dry weight was dominated by mussels (89.6% of total biomass) and crustaceans (8.4%).

3.2.3.1 Macrofauna

Macrofaunal taxa were represented by seven major taxonomic groups: Crustacea, Echinodermata (Ophiuridae), Gastropoda, Mytilidae, Polynoidae and other Polychaeta, and Pycnogonida. Total mean macrofaunal density was 12418 ± 9185 ind./m² for mean total dry weight of 925.9 ± 392.9 g/m².

Densities were dominated by *B. azoricus* (mean: 5620 ± 7445 ind./m² or 78.8% of the total macrofaunal density), followed by non-polynoid polychaetes (mean: 540 ± 1782 ind./m² or 7.6% of total macrofaunal density), gastropods (mean: 401 ± 823 ind./m² (5.6% total

macrofaunal density), crustaceans (mean : 364 ± 1368 ind./m²), polynoids (mean: 154 ± 476 ind./m² or 2.2% of total macrofaunal density), pycnogonids (mean: 46 ± 231 ind./m² or 0.6% of macrofaunal total density), and echinoderms (mean: 5 ± 16 ind./m² , less than 0.1% of macrofaunal total density).

Mussels dominated macrofaunal dry weight to an even greater extent with 89.9% of mean total dry weight (mean: 608.6 ± 356.2 g dry weight /m²). They were followed by crustaceans (mean: 57 ± 143 g dry weight/m² or 8.4% of total mean dry weight), polynoids (mean: 8.5 ± 26.2 g dry weight/m², 1.6 % of total mean dry weight), and, constituting less than 1% of the biomass: other polychaetes (mean: 2 ± 7.6 g dry weight/m² in average), gastropods (0.4 ± 0.6 g dry weight/m²), pycnogonids (mean: 0.2 ± 0.4 g dry weight/m²) and echinoderms (mean: 0.07 ± 0.2 g dry weight/m²).

3.2.3.2 Meiofauna

Meiofauna were represented by two main taxa: Nematoda and Copepoda. Nematodes dominated meiofaunal densities (90.4 %) with $13\,383 \pm 52\,932$ ind./m², while copepods reached a mean of 1425 ± 6187 ind./m² (9.6 %). Biomass showed the reverse pattern, with only $2.1 \times 10^{-3} \pm 8.6 \times 10^{-3}$ g dry weight/m² versus 14.3 ± 22.8 g dry weight/m² for nematodes and copepods, respectively.

3.2.4 Community biomass along the thermal gradient

The density of macrofaunal species varied along the thermal gradient (Figure 5A). The highest total density was observed in sample 05_3, with $38\,370$ ind./m², whereas the second densest sample was 06_12 with $23\,908$ ind./m². Both samples were from relatively cold habitats with temperatures ranging from 4.55 to 6.97°C. A group of eight other samples had

similar total density values, ranging from 8836 (06_4) to 15 958 (06_5) ind./m². The six remaining samples had the lowest densities ranging from 1600 (05_1) to 4580 ind./m² (05_5). These samples included those from the warmest habitats (temperatures from 4.75 to 14.19°C; 06_2, 06_6, 06_8, 06_10, 05_5) as well as the site with the lowest minimum temperature (05_1 with 3.73°C). Crustaceans tended to dominate on the left-hand side of the PCA-community, showing preferences for warm and unstable environments. The right-hand side of the PCA was dominated by mussels, gastropods and polychaetes, the latter being often dominant in the lower right-hand part of the plot, indicating a preference for relatively high minimum temperatures. Meiofauna were observed in densities greater than 10⁵ ind./m² in five cold samples: 06_4 (1.61x10⁵ ind./m²), 06_11 (2.97x10⁵ ind./m²), 06_1 (3.13x10⁵ ind./m²), 06_3 (5.67x10⁵ ind./m²), and 06_5 (5.98x10⁵ ind./m²). Other sample densities ranged from 0 individuals (05_4) to 8.8x10⁴ ind./m². Copepods dominated in only three intermediate to warm habitats, while nematodes dominated meiofaunal densities in the other samples (Figure 5B).

However, in terms of biomass, differences between both ends of the gradient and dominance in each sample changed (Figures 5C, D). Total biomass of macrofauna was maximal in sample 05_3 with 1490 g dry weight/m². Five other samples showed macrofaunal biomass above 1 kg dry weight/m²: 06_2 and 06_8, both corresponding to warm habitats (Table 2), and 06_9, 06_11 and 06_12, located in the cooler part of the PCA plot. The lowest biomass occurred at 05_1, a cold habitat, and 05_5, a warm habitat, with respectively 96 and 280 g dry weight/m². All other samples ranged from 519 to 967 g dry weight/m². Mussels were the main contributors to the dry weight in 14 of the 17 sites (82%). Shrimp dominated warm samples in terms of density (06_6, 06_2 and 06_8) but mussels dominated in terms of biomass. Shrimp and polynoids represented the second highest dry weights in samples, with shrimp more frequently dominating the lower part of the plot in higher minimal temperatures, whereas polynoids tended to dominate in areas where minimum temperatures are colder. Meiofaunal

biomass ranged from 0 to 13.7 g dry weight/m², except for three samples in the intermediate to cold habitats: 06_4 (31.3 g dry weight/m²), 06_3 (57.7 g dry weight/m²) and 06_5 (82.5 g dry weight/m²). Meiofaunal biomass dominance patterns were the opposite of those for density, with copepods constituting practically the totality of the meiofaunal dry weights in 15 of the 17 sites (Figure 5D).

3.2.5 Similarities between mussel size classes and the community niches

To look for taxon associations with the different mussel size classes, total mussel densities were replaced by densities of size classes obtained by the first niche similarity test (SIM-mussel). Tol and Rtol, two parameters of the OMI analysis, are null if the species is observed only once. To avoid associations based only on their observed frequency among the sites, Tol and Rtol were removed. The OMI parameter is a distance and carries the same information as centroid coordinates. Thus, species were simply clustered based on their coordinates in the niche analysis plot.

Niche analyses (OMI-community, Table 1) revealed that the residual tolerances of taxa observed in more than one sample ranged from 0.7% to 42% of total inertia, indicating that temperature explains 58 to 99.3% of their variance in distribution. Residual tolerances were greater than 50% of total inertia for 8 of the 78 taxa, indicating that temperature variables do not suffice to explain their niches: Amphipods (Rtol=71.4%), Dirivultids (Rtol=68.3%), *M. fortunata* (Rtol=57.6%), Ophriotrocha (Rtol=51.5%), Ostracoda (Rtol=84.4%), unidentified polynoids (Rtol=63.1%), Pseudotachidiidae (Rtol=67.4%) and *Segonzacia mesatlantica* (Rtol=96.5%). Permutation tests show significant marginality (OMI values) for only a few taxa: unidentified Alvinocaridiids, large mussels (shell lengths >60 mm) and small mussels (shell lengths <15 mm). This result indicates that these taxa are not distributed independently of their environment. Clustering (HC-community) identified four groups (corresponding to the four colours in Figure 6). Three of these groups were characterised by coordinates indicating

a niche in warmer habitats (brown, red and orange in Figure 6). The first was composed only of *Calomicrolaimus* nematodes, which differ from other taxa by a strong preference for the warmest habitats (Table 6, Figure 6, in brown). The second cluster (Table 7a, Figure 6, in red) was also characterised by centroid coordinates in warm thermal conditions, but to a lesser extent, and in particular includes large mussels and two species of shrimp. The third cluster (Table 7b, Figure 6, in orange) was composed of taxa whose centroids are situated in habitats with higher minima than other taxa, and especially includes *M. fortunata* shrimp and gastropods such as *Shinkaleipas briandi* and *Laeviphitus desbruyeresi*. The fourth and last cluster (Table 7c, Figure 6, in blue), characterised by cooler thermal conditions, included all the other species, in particular small and medium *B. azoricus*. Similarity tests (SIM-community, Figure 6) revealed numerous similar niches along the gradient. The six taxa located in the coldest habitats (*Theristus*, Cnidaria, Tanaidacea, *Lurifax vitreux*, *Lirapex costellata* and *Epsilonema*, lower left-hand part of Figure 6) share a similar niche between themselves, and with no other taxa of the same cluster (cluster 4), except the crab *S. mesatlantica* (Figure 6). The rest of taxa from this cluster shared similar niches but with no particular patterns. When excluding small and medium mussels, the 56 taxa composing the fourth cluster (in blue in Figure 6) showed 399 similar niches, which means that each taxon shares a similar niche with on average approximately 7 other taxa ($399/56$). Small *B. azoricus* shared a similar niche with 22 other taxa, and the niche of medium mussels was similar to that of 15 other taxa. Taxa from cluster 3 (in orange in Figure 6) can predict the presence of taxa coming both from clusters 3 and 4. The 12 taxa showed 51 similarities, which gave a ratio of 4.25 similarities per taxon. In cluster 2 (in red in Figure 6), larger mussels, unidentified Alvinocaridiidae shrimp and *Lepidonotopodium jouinae* polynoids showed similar niches with *Halomonhystera* nematodes (from cluster 4). All other similarities occurred among the taxa of cluster 2. For six taxa (larger mussels are excluded from the calculation), there were nine similar niches, giving a ratio of 1.5 similarities per taxon. The niche of large mussels was only similar to *Halomonhystera* and unidentified Alvinocaridiidae

while that of *Calomicrolaimus* (cluster 1, in brown in Figure 6) was only similar to unidentified Alvinocaridiidae (Figure 6).

4 Discussion

Here, we used novel statistical approaches to assess the thermal and biotic niche descriptors of the vent mussel *Bathymodiolus azoricus*, and of its associated species. Biomass of the assemblages on the edifice was determined for the first time for most of the species inventoried on the LS edifice Eiffel Tower. Our approach revealed that there is a link between mussel size structure and community composition as well as abiotic conditions. Our results provide insight on the success and role of *B. azoricus* in ecosystem functioning.

4.1 Niche of *Bathymodiolus azoricus*

In hydrothermal ecosystems, temperature is strongly linked with the hydrothermal fluid mixing gradient. Therefore, understanding the thermal niche of a species can give insight into its spatial distribution. *B. azoricus* was found in relatively cold waters, with mean temperatures ranging from 4.8 and 8.8°C for a maximum of 14.2°C. This range and maxima is similar to those reported in Sarrazin et al. (2015) and widens the thermal niche described in Cuvelier et al. (2011b). Here, we confirmed that — as revealed in Sarrazin et al. (2015) and Cuvelier et al. (2011b) — there are two or three microhabitats with a warmer, more variable environment and a colder, more stable environment.

This study demonstrated the previously reported fact (e.g. Comtet and Desbruyeres, 1998; Cuvelier et al., 2009) that the mussel thermal niche changes with mussel size (Figure 7).

Temperature, together with total dissolved sulphide and iron concentrations, are higher and more variable around larger mussel assemblages, with total dissolved sulphides reaching $40.07 \pm 25.16 \mu\text{mol/L}$ and total dissolved iron $5.25 \pm 3.60 \mu\text{mol/L}$ (Sarrazin et al., 2015). Smaller mussels are found in colder, more stable microhabitats and larger mussels colonise warmer, more variable microhabitats. Hence, large mussels appear to be better adapted to cope with greater abiotic variation. Our study is the first to take into account the breadth of the niche: each niche seems to partially overlap with neighbouring size categories, but the smallest (S1) and largest (S16) categories appear to be distinct. Both extreme size classes showed narrow ranges of temperatures, indicating specialist profiles. In contrast, mussels with intermediate shell lengths were observed in a broader range of habitats, suggesting a more generalist profile. This habitat preference pattern may indicate progressive acclimation of the mussels to warmer habitats and then selection of warmer habitats over colder ones by larger mussels. Niche similarity tests revealed that juveniles and mussels of less than 15 mm shared a similar niche, which is consistent with the size limits of mussel assemblages described in Cuvelier et al. (2009).

Juvenile mussel positioning along the thermal gradient can give some clues on the causes of thermal segregation. They were mainly observed in cold habitats, suggesting that these habitats are either more suitable for mussel growth during their youngest stages and/or that warmer habitats are relatively hostile for juvenile survival. Similarly, Gollner et al. (2015a) reported higher densities of juveniles on basalts, suggesting increasing energy requirements with growth, and migration to warmer habitats.

Several abiotic factors can limit juvenile settlement and growth in warmer habitats. Temperature *per se* is a strong limiting factor (Cuvelier et al., 2011b), but it is also strongly linked to the presence of toxic compounds, such as oxygen radicals that can be formed after

a redox reaction (Bebianno et al., 2005; Company et al., 2008), or metal and arsenic concentrations that can be filtered by mussels (Martins et al., 2011; Taylor et al., 2012). In addition, high fluctuations in the hydrothermal/seawater mixing ratio may be the cause of hypoxic periods for *B. azoricus*, which settles at the interface of the two fluids. Although *B. azoricus* was found to thrive in cooler waters, larger mussels in warmer habitats are more likely to experience hypoxia, compared to smaller mussels in cooler habitats.

Biotic factors were suggested to limit juvenile mussel recruitment in warmer habitats. These factors may include settlement inhibition and competition with other species, as observed along the East Pacific Ridge (EPR) (Lenihan et al., 2008), or with adult mussels (Comtet and Desbruyeres, 1998), or predation on larvae through grazing (Sancho et al., 2005), as observed in intertidal coastal environments (Dayton, 1971).

Differences in shell length between warm and cold habitats can be explained by two, non-exclusive hypotheses. The first hypothesis is that this segregation is the result of differences in growth efficiency of the different available food sources, as mentioned by Cuvelier et al. (2009), and as hypothesized by Bergquist et al. (2004). One model (Le Bris and Duperron, 2010) suggests that the available chemical energy increases along the mixing gradient of LS. In particular, basaltic sites such as the Eiffel Tower edifice are enriched in sulphides, and most of the energy available likely comes from sulphide oxidation (Perner et al., 2013). Methane oxidation may only be a secondary pathway on this edifice (Le Bris and Duperron, 2010). Larger mussels, living closer to the hydrothermal fluid emissions (Figure 7), have access to higher concentrations of both sulphides and methane and thus benefit from potentially higher energy sources than smaller mussels. Their large gill volumes can host a higher number of symbionts, enabling them to exploit a habitat with more reduced compounds and also to reduce the toxicity of this habitat.

The second hypothesis to explain differences in distribution is that the mussels can migrate to reach more suitable habitats. According to the distances of mussels to black smokers described in Cuvelier et al (2009), surfaces in close proximity to the fluid, offering higher potential productivity, represent areas of less than 8 m² (Figure 7). This may involve strong interspecific competition for space, for which larger mussels may be more competitive, owing to their larger gills, which may facilitate oxygen uptake in hypoxic habitats. The patchiness of the mussel beds at Eiffel Tower (Cuvelier et al., 2009) and the high spatial variability of physico-chemical conditions lead to the presence of an ensemble of niches separated by short distances, allowing short-range mussel movements. In addition, long-range migration (>10 cm) has already been observed for this species by video analysis (Sarrazin et al., 2014) and for other bathymodiolins (Govenar et al., 2004).

This change in thermal habitats highlights a more global change in the mussel niche as mussels grow. Several vent studies (e.g. Charlou et al., 2000) have shown that temperature is strongly correlated with several chemical compounds including those essential for chemosynthesis. Therefore, the presence of large mussels in warm temperature habitats is consistent with previous results (De Busserolles et al., 2009) highlighting changes in trophic diet, from a preferentially sulphide-based nutrition for smaller mussels to a preferentially methane-based nutrition for larger ones. It is also consistent with results (Martins et al., 2008) hypothesizing a shift from particle filtration in small mussels to symbiotic food sources in larger individuals.

Length-age relationships would help better understand habitat selection by vent *Bathymodiolus* mussels. Such data can be obtained using *in situ* fluorochrome staining chambers on deep-sea bivalves. Recent studies demonstrate semi-diurnal shell growth

rates: *Bathymodiolus brevior* (Schöne and Giere, 2005); *Calyptogena soyoae* and *Calyptogena okutanii* (Tada et al., 2009); *Bathymodiolus thermophilus* (Nedoncelle et al., 2013); and *B. thermophilus* and *B. azoricus* (Nedoncelle et al., 2014). Indeed, results of these studies were included in Von Bertalanffy growth models, all showing a higher growth rate for smaller mussels, which discards our first hypothesis of differential growth for *B. azoricus* to explain spatial size segregation.

4.2 Niches of associated species

The study of species' thermal niches can be used to further understand their spatial variation. Niche analyses revealed that temperature is a useful variable for describing the niche of a large majority of the associated species studied (nearly 90%). Nevertheless, it was insufficient for describing the niche of Amphipods, Dirivultids, *Mirocaris fortunata*, Ophriotrocha, Ostracoda, unidentified polynoids, Pseudotachidiidae and *Segonzacia mesatlantica*, which high mobility can allow to cope easily with thermal variability. For these species, niches would be better explained by variables other than temperature, such as the type of substratum, or the presence of a food source. For example, for Dirivultids, their success in various hydrothermal contexts confirms their broad tolerance to thermal variability (Gollner et al., 2010b). Only unidentified Alvinocaridids, large mussels (shell lengths >60 mm) and small mussels (shell lengths <15 mm), have been found to have significantly marginal thermal niches, i.e. their global thermal environment is different from that of most of the other taxa of mussel assemblages. For the rest of the community, clusters were distributed along the gradient, differing more in their optimal maximum temperatures than in their average or minimum temperatures. Several vent studies have started to propose that, aside from mean environmental conditions, the distribution of the hydrothermal community depends on environmental variation (Cuvelier et al., 2011b; Sarrazin et al., 2006; Sen et al., 2013). For example, Gollner et al. (2015b) suggested that the different distribution of

meiofauna and macrofauna can be explained by the macrofaunal ability to develop protection against environmental variations such as thick shells.

B. azoricus macrofaunal communities were dominated in density by the mussels themselves, by Crustacea, mainly represented by *M. fortunata* shrimp, and by Polychaeta, particularly polynoids such as *Branchipolynoe seepensis*. Crustaceans tend to dominate in warmer habitats, polychaetes in habitats with higher thermal minima, and mussels in colder habitats. Gastropods such as *Lepetodrilus atlanticus*, *Protolira valvatoides* or polynoids such as the mussel-associated species *B. seepensis*, often constitute the second highest species density in colder habitats. All three species have been identified as species indicative of cold habitats (Sarrazin et al., 2015). In comparison, ophiroid and pycnogonid densities were much lower. Nematoda dominated the the meiofaunal densities on LS, as was found by Zekely et al. (2006) on MAR. They tend to dominate in colder habitats while Copepoda tended to dominate in warmer habitats. Overall densities of meiofauna were higher in colder habitats. Similarly, Galkin and Goroslavskaya (2010) observed two types of *B. azoricus* assemblages: those dominated by nematodes and those dominated by copepods. On the Juan de Fuca ridge, Tsurumi et al. (2003) also found that copepods show higher densities in warmer habitats. Likewise, Gollner et al. (2010a) observed more copepods in the warm pompeii worm community, while mussel communities showed similar proportions of nematodes and copepods.

Niche similarity tests showed that the coldest habitats were inhabited by the Cnidaria, with only a few species having a similar niche. A peripheral assemblage of anemones is also found on several other edifices (Colaço et al., 1998; Marsh et al., 2012). Small and medium mussels had niches similar to numerous other species in the colder habitats. For some of these species, niche similarities can be explained easily. For example, both size classes

have a niche similar to ophiuroids, which may feed on mussel pseudo faeces (Desbruyeres et al., 2006). They also have a niche similar to *Amathys lutzi*, a bacterivorous polychaete (Colaço et al., 2002) which is explained by the fact that they create tubes in the byssus of mussels. Most of the species sharing the same niche as small and medium mussels were detritivores, e.g. pycnogonids, *Protolira valvatoides* (Desbruyeres et al., 2006), or bacterial mat grazers, e.g. *Lepetodrilus atlanticus* (Desbruyeres et al., 2006). Contrastingly, taxa inhabiting warmer habitats were more often carnivorous: e.g. Porifera or *Lepidonotopodium jouinae* (Desbruyères et al 2006), or feed on free-living bacteria such as *Chorocaris chacei* and *M. fortunata*. *Branchinotogluma* species, which can feed on shrimp or graze bacterial mats (Desbruyeres et al., 2006), were found in both habitats. Levesque et al. (2006), Limén et al. (2008) and De Busserolles et al. (2009) observed intraspecific spatial variation in species' diets. Combinations of results from niche similarity tests and presence/absence data may highlight interactions between species and further assess the factors influencing their distribution along the thermal gradient.

4.3 Biomass and implications in ecosystem functioning

Biomass values in this study were in the range of previously studied hydrothermal ecosystems. Total biomass analysis revealed that about one-third of the samples have a biomass exceeding 1 kg in dry weight per square meter. In addition, in the MoMARSAT 2014 samples, which were not included in the total biomass analyses, mussel biomass alone reached more than 3 kg dry weight per square meter. Total community biomass on the LS Eiffel Tower edifice may therefore reach more than 3 kg dry weight per square meter. Similarly, other studies on biomass show ranges from less than 1 kg dry weight/m² to over 4.7 kg dry weight/m² (Juan de Fuca tubeworm field, Sarrazin and Juniper, 1999). Mussel assemblages on Logatchev reached 70 kg wet weight with shell/m² (Gebruk et al., 2000). Hypothesising that the shape of *B. azoricus* and *B. puteoserpensis* species are similar, and

considering that mussel shell-free dry weight is about 5.8% of its wet weight with shell, the biomass on Logatchev would reach approximately 4.06 kg dry weight/m². Nevertheless, LS mussel assemblages reach a mean biomass greater than high-temperature alvinellid assemblages of Juan de Fuca Ridge, and most photosynthesis-based marine faunal ecosystems (Sarrazin and Juniper, 1999, and references therein).

In contrast to the density results, there was no clear pattern of biomass along the thermal gradient (Figure 7). High biomass levels were found alternately in higher and lower temperature microhabitats. These differences are unlikely due to variables such as sulphide or iron concentrations, because they are strongly correlated with temperature. Therefore, factors explaining the distribution of mussel biomass and that of their associated species should be explored for parameters non-correlated with temperature, such as geomorphological features or successional history. *B. azoricus* constituted in average almost 90% of total biomass per square meter. Its success along the hydrothermal fluid gradient is most probably linked to its singular biology. Its dual symbiosis and ability to filter toxic substances provide the mussel with high trophic plasticity (Duperron et al., 2006; Fiala-Médioni et al., 2002; Riou et al., 2010). In addition, the relative proportion of chemosynthetic symbionts is somehow linked to the ambient physical and chemical conditions (Halary et al., 2008; Le Bris and Duperron, 2010), suggesting that they can adapt to temporal changes (Kádár et al., 2005). *B. azoricus* is thus able to cope with highly variable temporal and spatial environmental conditions, such as those observed in the warm vent habitats. Other studies have highlighted the dominance in biomass of symbiont-bearing species in hydrothermal ecosystems around the globe (e.g. Sen et al., 2013)

The study of biomass in an ecosystem provides various insights on its functioning. The relationship between biomass and species richness is a widely used, albeit debated, topic in

ecosystem studies. It can help clarify potential biotic interactions along the thermal gradient. Colder habitats harbour high diversity and sometimes high biomass. Some studies attribute this relationship to a higher degree of resource partitioning between taxa (Tilman et al., 1997). Others suggest niche and fitness differences between the taxa (Carroll et al., 2011). In contrast, in warmer habitats, diversity was lower for an equivalent amount of biomass. This pattern suggests that colonisation is limited by environmental toxicity, and/or high degree of competition in this part of the gradient, where available substrate may be scarce (Figure 7).

The study of biomass is also a way to assess the available organic carbon of an ecosystem. In addition to its trophic plasticity, *B. azoricus* has few known predators except the crab *Segonzacia mesatlantica*, a supposed scavenger of the mussel (Colaço et al., 2002; De Busserolles et al., 2009), which may further explain its success on the edifice. The mussel constitutes, with its commensal polychaete species *B. seepensis*, an independent trophic group (De Busserolles et al., 2009). Its importance, in terms of biomass, and the fact that it seems to represent a trophic dead-end raises the question of the fate of *B. azoricus* organic carbon. The organic carbon excreted by the mussel or included in dead mussels may be carried away from the edifice by hydrodynamic processes. Few data are currently available on the carbon accessible in the water surrounding the mussel beds and in the neighbouring deep-sea habitats. Sarradin et al. (1998) reported high levels of dissolved organic carbon (DOC) of up to 600 $\mu\text{mol/L}$ in the fluid surrounding the mussels. Particulate organic carbon fluxes have been measured by Khripounoff et al. (2008) at the base of another active edifice of the LS vent field where they reach a mean of 131 $\text{mg/m}^2/\text{d}$ (ranging from 52 to 308 $\text{mg/m}^2/\text{d}$). Alternatively, particles are carried away from the edifice and fall on the seafloor. Sediment samples were taken at the base of Eiffel Tower edifice during the MoMARSAT 2014 cruise and sieved. Preliminary results showed that only around 5% of dry weight was organic matter, which may suggest that organic matter exports from the edifice are limited, implying high organic carbon turnover rates by the vent community.

4.5 Analytical approach: advantages, limitations and potential

Temperature proved to be a good factor for identifying differences in species habitats on the Eiffel Tower edifice. As temperature is strongly linked to fluid chemistry, the niches may also be defined by other variables, such as reduced or toxic compounds concentrations. However, Podowski et al. (2010) found that temperature, rather than sulphide, limits the distribution of symbiotic fauna, such as *Ifremeria nautiliei* and *Alviniconcha* spp. at Lau Basin (Pacific Ocean). When fluid physico-chemical characteristics are not relevant to define a species realized niche, one can consider other factors such as mobility or competition (Sen et al., 2013).

The OMI analysis detected multimodal, non-linear distributions of species across temperature variables. In contrast, classical multivariate niche analyses such as canonical or redundancy analyses rely on multimodal or linear distributions of species. OMI analysis can explain more data variability than the two other methods (Dolédec et al., 2000). It can also be used to assess niche breadth through the tolerance ("Tol") parameter. As for any other multivariate analysis, however, especially when analysing species distribution, OMI requires a sufficient number of samples that have been collected across the entire gradient of the faunal assemblages. For this study, sites were sampled during three different cruises. Among them, only one cruise (MoMARSAT 2014) had a sampling protocol specifically designed for this study. The samples in this analysis were therefore not homogeneous and colder habitats were better represented. However, the compilation of data from different cruises allowed us to study all the faunal assemblages available for the Eiffel Tower edifice. Furthermore, the number of samples from the warm habitats is proportional to their frequency: they occupy a much smaller surface on the edifice (Figure 7) than the cold habitats (Cuvelier et al., 2009). This heterogeneity in sampling partially explains the

differences in the results of the clustering and niche similarity analyses on mussel size categories.

Clustering and niche similarity tests were complementary approaches. The hierarchical clustering method outputs clusters of taxa that experience the same thermal conditions, and, more interestingly, highlight how these clusters differ from each other. On the other hand, similarity tests take the analysis further by revealing which taxa share niche conditions more than expected by chance. In other words, it tests and details the clustering. Performing the similarity test without the cluster analysis would not provide any information on how the niches differ. However, the differences in the grouping pattern according to mussel size class raises an intriguing question. In the clustering analysis, the distinction between small and intermediate shell lengths was approximately 35 mm, with mussels smaller than this value sharing a similar environment. In contrast, the niche similarity analysis conducted on size categories grouped small mussels from 5 to 15 mm in length. Both analyses defined the limit between intermediate and large mussels at between 60 and 70 mm. One explanation lies in the sampling. The ecological objectives of the EXOMAR cruise specifically targeted small mussel assemblages, from five closely located samples. Therefore, more than 75% of the shells were below the 35 mm limit. Because the samples were close to each other, it is quite likely that the mussels experience the same thermal conditions, which explains that the clustering analysis placed most of mussel lengths below 35 mm in the same thermal conditions. Also, a tolerance parameter was included in the clustering analysis, and tolerance for mussels belonging to S1 (minimum 5 mm) to S7 (maximum 35 mm) were smaller than for larger mussels, which may have favored their clustering.

The integration of several cruises in the same analytical framework also illustrated the importance of replicate sampling, even on a single edifice. A total of 41 taxa were sampled

during the EXOMAR cruise (n=5) whereas the MOMARETO cruise doubled this number (71 taxa) with double the number of samples (n=12). Out of the total number of taxa (78), 42% were observed in only one or two samples, indicating that there are numerous rare taxa in the samples. This number is slightly higher than that observed by Sarrazin et al. (2015) with only the MOMARETO samples (39%). Moreover, 15% of the taxa sampled during EXOMAR were not sampled again during MOMARETO. Thus, even after 28 cruises and over 15 years of exploration, sampling remains a focal point. More samples are needed as is the development of new quantitative sampling procedures for an exhaustive overview of the edifice community.

Conclusion

The analysis of data originating from several cruises using a novel statistical framework resulted in the corroboration of previously observed spatial segregation of the vent mussel *B. azoricus*, and the observation of a change in its niche breadth. This study also confirms the observation of a gradual change in community structure along the thermal gradient and supports De Busserolles et al. (2009) results showing diet changes with mussel size categories along this gradient. Thermal variability, rather than environmental average conditions, seem to drive species distribution. This study also contributed to the description of marine biodiversity: it updated the Eiffel Tower species list on the LS vent field and biomass of the community was evaluated for the first time. These results provided insight into the functioning of these ecosystems and on the role *B. azoricus* may have in its community. All of these data are essential to contribute to ecosystem modelling which is a useful tool for designing management strategy plans for the sustainable exploitation of the deep ocean.

5 Acknowledgements

We would like to thank the crews and captains Phillipe Guillemet, Thierry Alix et Gilles Ferrand of the French vessels *Pourquoi Pas?* and *L'Atalante* for their cooperation and assistance in the success of the four cruises described in this study (EXOMAR, MOMARETO, MoMARSAT 2011 and 2014). We would also like to thank all ROV *Victor 6000* pilots for their remarkable work in helping us gathering these data. We are grateful to Daphné Cuvelier for her unconditional help on this edifice she knows so well. We are also grateful to the LEP technical and engineering teams for their support at sea and in the laboratory. BH was supported by the "Laboratoire d'Excellence" LabexMER (ANR-10-LABX-19) and co-funded by a grant from the French government under the program "Investissements d'Avenir". The project is also part of the EMSO-Acores research programme funded by an ANR research grant (ANR Lucky Scales ANR-14-CE02-0008-02). The research leading to these results has also received funding from the European Union Seventh Framework Programme (FP7/2007-2013) under the MIDAS project, grant agreement n° 603418.

6 References

- Andrassy, I. (1956). Die rauminhalts-und gewichtsbestimmung der fadenwürmer (Nematoden). *Acta Zool. Hung.* 2, 1–5.
- Barreyre, T., Escartín, J., Garcia, R., Cannat, M., Mittelstaedt, E., and Prados, R. (2012). Structure, temporal evolution, and heat flux estimates from the Lucky Strike deep-sea hydrothermal field derived from seafloor image mosaics. *Geochem. Geophys. Geosystems* 13, Q04007.
- Bates, A.E., Lee, R.W., Tunnicliffe, V., and Lamare, M.D. (2010). Deep-sea hydrothermal vent animals seek cool fluids in a highly variable thermal environment. *Nat. Commun.* 1, 14.
- Bebianno, M.J., Company, R., Serafim, A., Camus, L., Cosson, R.P., and Fiala-Médoni, A. (2005). Antioxidant systems and lipid peroxidation in *Bathymodiolus azoricus* from Mid-Atlantic Ridge hydrothermal vent fields. *Aquat. Toxicol.* 75, 354–373.
- Bergquist, D.C., Fleckenstein, C., Szalai, E.B., Knisel, J., and Fisher, C.R. (2004). Environment drives physiological variability in the cold seep mussel *Bathymodiolus childressi*. *Limnol. Oceanogr.* 49, 706–715.

- Bergquist, D.C., Eckner, J.T., Urcuyo, I.A., Cordes, E.E., Hourdez, S., Macko, S.A., and Fisher, C.R. (2007). Using stable isotopes and quantitative community characteristics to determine a local hydrothermal vent food web. *Mar. Ecol. Prog. Ser.* *330*, 49–65.
- Broennimann, O., Fitzpatrick, M.C., Pearman, P.B., Petitpierre, B., Pellissier, L., Yoccoz, N.G., Thuiller, W., Fortin, M.-J., Randin, C., Zimmermann, N.E., et al. (2012). Measuring ecological niche overlap from occurrence and spatial environmental data. *Glob. Ecol. Biogeogr.* *21*, 481–497.
- Carroll, I.T., Cardinale, B.J., and Nisbet, R.M. (2011). Niche and fitness differences relate the maintenance of diversity to ecosystem function. *Ecology* *92*, 1157–1165.
- Charlou, J.L., Donval, J.P., Douville, E., Jean-Baptiste, P., Radford-Knoery, J., Fouquet, Y., Dapoigny, A., and Stievenard, M. (2000). Compared geochemical signatures and the evolution of Menez Gwen (37°50'N) and Lucky Strike (37°17'N) hydrothermal fluids, south of the Azores Triple Junction on the Mid-Atlantic Ridge. *Chem. Geol.* *171*, 49–75.
- Chase, J.M., and Leibold, M.A. (2003). *Ecological Niches: Linking Classical and Contemporary Approaches* (University of Chicago Press).
- Colaço, A., Desbruyères, D., Comtet, T., and Alayse, A.-M. (1998). Ecology of the Menez Gwen hydrothermal vent field (Mid-Atlantic Ridge/Azores Triple Junction). *Cah. Biol. Mar.* *39*, 237–240.
- Colaço, A., Dehairs, F., and Desbruyères, D. (2002). Nutritional relations of deep-sea hydrothermal fields at the Mid-Atlantic Ridge: a stable isotope approach. *Deep Sea Res. Part Oceanogr. Res. Pap.* *49*, 395–412.
- Colwell, R.K., and Futuyma, D.J. (1971). On the Measurement of Niche Breadth and Overlap. *Ecology* *52*, 567–576.
- Company, R., Serafim, A., Bebianno, M.J., Cosson, R., Shillito, B., and Fiala-Médioni, A. (2004). Effect of cadmium, copper and mercury on antioxidant enzyme activities and lipid peroxidation in the gills of the hydrothermal vent mussel *Bathymodiolus azoricus*. *Mar. Environ. Res.* *58*, 377–381.
- Company, R., Serafim, A., Cosson, R.P., Fiala-Médioni, A., Camus, L., Colaço, A., Serrão-Santos, R., and Bebianno, M.J. (2008). Antioxidant biochemical responses to long-term copper exposure in *Bathymodiolus azoricus* from Menez-Gwen hydrothermal vent. *Sci. Total Environ.* *389*, 407–417.
- Comtet, T., and Desbruyères, D. (1998). Population structure and recruitment in mytilid bivalves from the Lucky Strike and Menez Gwen. *Mar. Ecol. Prog. Ser.* *163*, 165–177.
- Copley, J.T.P., Tyler, P.A., Murton, B.J., and Van Dover, C.L. (1997). Spatial and interannual variation in the faunal distribution at Broken Spur vent field (29 N, Mid-Atlantic Ridge). *Mar. Biol.* *129*, 723–733.
- Copley, J.T.P., Jorgensen, P.B.K., and Sohn, R.A. (2007). Assessment of decadal-scale ecological change at a deep Mid-Atlantic hydrothermal vent and reproductive time-series in the shrimp *Rimicaris exoculata*. *J. Mar. Biol. Assoc. U. K.* *87*, 859–867.
- Corliss, J.B., Dymond, J., Gordon, L.I., Edmond, J.M., von Herzen, R.P., Ballard, R.D., Green, K., Williams, D., Bainbridge, A., Crane, K., et al. (1979). Submarine Thermal Springs on the Galapagos Rift. *Science* *203*, 1073–1083.

- Cuvelier, D., Sarrazin, J., Colaço, A., Copley, J., Desbruyères, D., Glover, A.G., Tyler, P., and Serrão Santos, R. (2009). Distribution and spatial variation of hydrothermal faunal assemblages at Lucky Strike (Mid-Atlantic Ridge) revealed by high-resolution video image analysis. *Deep Sea Res. Part Oceanogr. Res. Pap.* *56*, 2026–2040.
- Cuvelier, D., Sarrazin, J., Colaço, A., Copley, J.T., Glover, A.G., Tyler, P.A., Santos, R.S., and Desbruyères, D. (2011a). Community dynamics over 14 years at the Eiffel Tower hydrothermal edifice on the Mid-Atlantic Ridge. *Limnol. Oceanogr.* *56*, 1624–1640.
- Cuvelier, D., Sarradin, P.-M., Sarrazin, J., Colaço, A., Copley, J.T., Desbruyères, D., Glover, A.G., Santos, R.S., and Tyler, P.A. (2011b). Hydrothermal faunal assemblages and habitat characterisation at the Eiffel Tower edifice (Lucky Strike, Mid-Atlantic Ridge). *Mar. Ecol.* *32*, 243–255.
- Cuvelier, D., De Busserolles, F., Lavaud, R., Floc'h, E., Fabri, M.-C., Sarradin, P.-M., and Sarrazin, J. (2012). Biological data extraction from imagery—How far can we go? A case study from the Mid-Atlantic Ridge. *Mar. Environ. Res.* *82*, 15–27.
- Dayton, P.K. (1971). Competition, Disturbance, and Community Organization: The Provision and Subsequent Utilization of Space in a Rocky Intertidal Community. *Ecol. Monogr.* *41*, 351–389.
- De Busserolles, F., Sarrazin, J., Gauthier, O., Gélinas, Y., Fabri, M.C., Sarradin, P.M., and Desbruyères, D. (2009). Are spatial variations in the diets of hydrothermal fauna linked to local environmental conditions? *Deep Sea Res. Part II Top. Stud. Oceanogr.* *56*, 1649–1664.
- Desbruyères, D., Biscoito, M., Caprais, J.-C., Colaço, A., Comtet, T., Crassous, P., Fouquet, Y., Khrifounoff, A., Le Bris, N., Olu, K., et al. (2001). Variations in deep-sea hydrothermal vent communities on the Mid-Atlantic Ridge near the Azores plateau. *Deep Sea Res. Part Oceanogr. Res. Pap.* *48*, 1325–1346.
- Desbruyères, D., Segonzac, M., and Bright, M. (2006). *Handbook of Deep-Sea Hydrothermal Vent Fauna*. Linz. Austria Biol.
- Dolédec, S., Chessel, D., and Gimaret-Carpentier, C. (2000). Niche separation in community analysis: a new method. *Ecology* *81*, 2914–2927.
- Dray, S., Dufour, A.-B., and others (2007). The ade4 package: implementing the duality diagram for ecologists. *J. Stat. Softw.* *22*, 1–20.
- Duong, T. (2015). *ks: Kernel Smoothing*.
- Duperron, S., Bergin, C., Zielinski, F., Blazejak, A., Pernthaler, A., McKiness, Z.P., DeChaine, E., Cavanaugh, C.M., and Dubilier, N. (2006). A dual symbiosis shared by two mussel species, *Bathymodiolus azoricus* and *Bathymodiolus puteoserpentis* (Bivalvia: Mytilidae), from hydrothermal vents along the northern Mid-Atlantic Ridge. *Environ. Microbiol.* *8*, 1441–1447.
- Elton, C. (1927). *Animal Ecology*, 1927. Sidgwick Jackson LTD Lond.
- Fabri, M.-C., Bargain, A., Briand, P., Gebruk, A., Fouquet, Y., Morineaux, M., and Desbruyères, D. (2011). The hydrothermal vent community of a new deep-sea field, Ashadze-1, 12 58' N on the Mid-Atlantic Ridge. *J. Mar. Biol. Assoc. U. K.* *91*, 1–13.
- Fiala-Médioni, A., McKiness, Z., Dando, P., Boulegue, J., Mariotti, A., Alayse-Danet, A., Robinson, J., and Cavanaugh, C. (2002). Ultrastructural, biochemical, and immunological characterization of two

populations of the mytilid mussel *Bathymodiolus azoricus* from the Mid-Atlantic Ridge: evidence for a dual symbiosis. *Mar. Biol.* *141*, 1035–1043.

Galkin, S.V., and Goroslavskaya, E.I. (2010). Bottom fauna associated with *Bathymodiolus azoricus* (Mytilidae) mussel beds in the hydrothermal fields of the Mid-Atlantic Ridge. *Oceanology* *50*, 51–60.

Gaudron, S.M., Lefebvre, S., Nunes Jorge, A., Gaill, F., and Pradillon, F. (2012). Spatial and temporal variations in food web structure from newly-opened habitat at hydrothermal vents. *Mar. Environ. Res.* *77*, 129–140.

Gebbruk, A.V., Chevalloné, P., Shank, T., Lutz, R.A., and Vrijenhoek, R.C. (2000). Deep-sea hydrothermal vent communities of the Logatchev area (14 45' N, Mid-Atlantic Ridge): Diverse biotopes and high biomass. *J. Mar. Biol. Assoc. UK* *80*, 383–393.

Gollner, S., Riemer, B., Arbizu, P.M., Le Bris, N., and Bright, M. (2010a). Diversity of meiofauna from the 9 50' N East Pacific Rise across a gradient of hydrothermal fluid emissions. *Plos One* *5*, e12321.

Gollner, S., Fontaneto, D., and Arbizu, P.M. (2010b). Molecular taxonomy confirms morphological classification of deep-sea hydrothermal vent copepods (Dirivultidae) and suggests broad physiological tolerance of species and frequent dispersal along ridges. *Mar. Biol.* *158*, 221–231.

Gollner, S., Govenar, B., Arbizu, P.M., Mills, S., Le Bris, N., Weinbauer, M., Shank, T.M., and Bright, M. (2015a). Differences in recovery between deep-sea hydrothermal vent and vent-proximate communities after a volcanic eruption. *Deep Sea Res. Part Oceanogr. Res. Pap.* *106*, 167–182.

Gollner, S., Govenar, B., Fisher, C.R., and Bright, M. (2015b). Size matters at deep-sea hydrothermal vents: different diversity and habitat fidelity patterns of meio- and macrofauna. *Mar. Ecol. Prog. Ser.* *520*, 57–66.

Govenar, B., Freeman, M., Bergquist, D.C., Johnson, G.A., and Fisher, C.R. (2004). Composition of a one-year-old *Riftia pachyptila* community following a clearance experiment: insight to succession patterns at deep-sea hydrothermal vents. *Biol. Bull.* *207*, 177–182.

Grelon, D., Morineaux, M., Desrosiers, G., and Juniper, S.K. (2006). Feeding and territorial behavior of *Paralvinella sulfincola*, a polychaete worm at deep-sea hydrothermal vents of the Northeast Pacific Ocean. *J. Exp. Mar. Biol. Ecol.* *329*, 174–186.

Grinnell, J. (1917). The Niche-Relationships of the California Thrasher. *The Auk* *34*, 427–433.

Halary, S., Riou, V., Gaill, F., Boudier, T., and Duperron, S. (2008). 3D FISH for the quantification of methane- and sulphur-oxidizing endosymbionts in bacteriocytes of the hydrothermal vent mussel *Bathymodiolus azoricus*. *ISME J.* *2*, 284–292.

Husson, F., Josse, J., Le, S., Mazet, J., and Husson, M.F. (2015). Package “FactoMineR.”

Hutchinson, G.E. (1957). Cold spring harbor symposium on quantitative biology. Concluding Remarks *22*, 415–427.

Kádár, E., Bettencourt, R., Costa, V., Santos, R.S., Lobo-da-Cunha, A., and Dando, P. (2005). Experimentally induced endosymbiont loss and re-acquirement in the hydrothermal vent bivalve *Bathymodiolus azoricus*. *J. Exp. Mar. Biol. Ecol.* *318*, 99–110.

- Khripounoff, A., Vangriesheim, A., Crassous, P., Segonzac, M., Lafon, V., and Warén, A. (2008). Temporal variation of currents, particulate flux and organism supply at two deep-sea hydrothermal fields of the Azores Triple Junction. *Deep Sea Res. Part Oceanogr. Res. Pap.* *55*, 532–551.
- Kim, S., and Hammerstrom, K. (2012). Hydrothermal vent community zonation along environmental gradients at the Lau back-arc spreading center. *Deep Sea Res. Part Oceanogr. Res. Pap.* *62*, 10–19.
- Langmuir, C., Humphris, S., Fornari, D., Van Dover, C., Von Damm, K., Tivey, M.K., Colodner, D., Charlou, J.-L., Desonie, D., Wilson, C., et al. (1997). Hydrothermal vents near a mantle hot spot: the Lucky Strike vent field at 37°N on the Mid-Atlantic Ridge. *Earth Planet. Sci. Lett.* *148*, 69–91.
- Le Bris, N., and Duperron, S. (2010). Chemosynthetic communities and biogeochemical energy pathways along the Mid-Atlantic Ridge: The case of *Bathymodiolus Azoricus*. In *Diversity Of Hydrothermal Systems On Slow Spreading Ocean Ridges*, P.A. Rona, C.W. Devey, J. Dymont, and B.J. Murton, eds. (American Geophysical Union), pp. 409–429.
- Le Bris, N., Rodier, P., Sarradin, P.-M., and Le Gall, C. (2006). Is temperature a good proxy for sulfide in hydrothermal vent habitats? *Cah. Biol. Mar.* *47*, 465–470.
- Lenihan, H.S., Mills, S.W., Mullineaux, L.S., Peterson, C.H., Fisher, C.R., and Micheli, F. (2008). Biotic interactions at hydrothermal vents: Recruitment inhibition by the mussel *Bathymodiolus thermophilus*. *Deep Sea Res. Part Oceanogr. Res. Pap.* *55*, 1707–1717.
- Léveillé, R.J., Levesque, C., and Juniper, S.K. (2005). Biotic Interactions and Feedback Processes in Deep-Sea Hydrothermal Vent Ecosystems. In *Interactions Between Macro- and Microorganisms in Marine Sediments*, E. Kristensen, R.R. Haese, and J.E. Kostka, eds. (American Geophysical Union), pp. 299–321.
- Levesque, C., Juniper, S.K., and Marcus, J. (2003). Food resource partitioning and competition among alvinellid polychaetes of Juan de Fuca Ridge hydrothermal vents. *Mar. Ecol. Prog. Ser.* *246*, 173–182.
- Levesque, C., Juniper, K., and Limén, H. (2006). Spatial organization of food webs along habitat gradients at deep-sea hydrothermal vents on Axial Volcano, Northeast Pacific. *Deep Sea Res. Part Oceanogr. Res. Pap.* *53*, 726–739.
- Limén, H., Stevens, C., Bourass, Z., and Juniper, S. (2008). Trophic ecology of siphonostomatoid copepods at deep-sea hydrothermal vents in the northeast Pacific. *Mar. Ecol. Prog. Ser.* *359*, 161–170.
- Luther, G.W., Rozan, T.F., Taillefert, M., Nuzzio, D.B., Di Meo, C., Shank, T.M., Lutz, R.A., and Cary, S.C. (2001). Chemical speciation drives hydrothermal vent ecology. *Nature* *410*, 813–816.
- Lutz, R.A., Shank, T.M., Luther, G.W., Vetrariani, C., Tolstoy, M., Nuzzio, D.B., Moore, T.S., Waldhauser, F., Crespo-Medina, M., Chatziefthimiou, A.D., et al. (2008). Interrelationships Between Vent Fluid Chemistry, Temperature, Seismic Activity, and Biological Community Structure at a Mussel-Dominated, Deep-Sea Hydrothermal Vent Along the East Pacific Rise. *J. Shellfish Res.* *27*, 177–190.
- Marsh, L., Copley, J.T., and Tyler, P.A. (2012). Microdistribution and reproductive ecology of *Kiwa* n. sp. associated with hydrothermal vent fields on the East Scotia Ridge, Southern Ocean.
- Martins, I., Colaço, A., Dando, P.R., Martins, I., Desbruyères, D., Sarradin, P.-M., Marques, J.C., and Serrão-Santos, R. (2008). Size-dependent variations on the nutritional pathway of *Bathymodiolus azoricus* demonstrated by a C-flux model. *Ecol. Model.* *217*, 59–71.

- Martins, I., Cosson, R.P., Riou, V., Sarradin, P.-M., Sarrazin, J., Santos, R.S., and Colaço, A. (2011). Relationship between metal levels in the vent mussel *Bathymodiolus azoricus* and local microhabitat chemical characteristics of Eiffel Tower (Lucky Strike). *Deep Sea Res. Part Oceanogr. Res. Pap.* *58*, 306–315.
- Matabos, M., Cuvelier, D., Brouard, J., Shillito, B., Ravaux, J., Zbinden, M., Barthelemy, D., Sarradin, P.M., and Sarrazin, J. (2015). Behavioural study of two hydrothermal crustacean decapods: *Mirocaris fortunata* and *Segonzacia mesatlantica*, from the Lucky Strike vent field (Mid-Atlantic Ridge). *Deep Sea Res. Part II Top. Stud. Oceanogr.* *121*, 146–158.
- McMullin, E.R., Bergquist, D.C., and Fisher, C.R. (2000). Metazoans in Extreme Environments: Adaptations of Hydrothermal Vent and Hydrocarbon Seep Fauna. *Gravitational Space Res.* *13*.
- Micheli, F., Peterson, C.H., Mullineaux, L.S., Fisher, C.R., Mills, S.W., Sancho, G., Johnson, G.A., and Lenihan, H.S. (2002). Predation structures communities at deep-sea hydrothermal vents. *Ecol. Monogr.* *72*, 365–382.
- Mullineaux, L.S., Peterson, C.H., Micheli, F., and Mills, S.W. (2003). Successional Mechanism Varies Along a Gradient in Hydrothermal Fluid Flux at Deep-Sea Vents. *Ecol. Monogr.* *73*, 523–542.
- Mullineaux, L.S., Adams, D.K., Mills, S.W., and Beaulieu, S.E. (2010). Larvae from afar colonize deep-sea hydrothermal vents after a catastrophic eruption. *Proc. Natl. Acad. Sci.* *107*, 7829–7834.
- Mullineaux, L.S., Le Bris, N., Mills, S.W., Henri, P., Bayer, S.R., Secrist, R.G., and Siu, N. (2012). Detecting the Influence of Initial Pioneers on Succession at Deep-Sea Vents. *PLoS ONE* *7*, e50015.
- Nedoncelle, K., Lartaud, F., De Rafelis, M., Boulila, S., and Le Bris, N. (2013). A new method for high-resolution bivalve growth rate studies in hydrothermal environments. *Mar. Biol.* *160*, 1427–1439.
- Nedoncelle, K., Le Bris, N., de Rafélis, M., Labourdette, N., and Lartaud, F. (2014). Non-equilibrium fractionation of stable carbon isotopes in chemosynthetic mussels. *Chem. Geol.* *387*, 35–46.
- Oksanen, J., Blanchet, F.G., Kindt, R., Legendre, P., Minchin, P.R., O'Hara, R.B., Simpson, G.L., Solymos, P., Stevens, M.H.H., Wagner, H., et al. (2015). Package “vegan.” *Community Ecol. Package Version 2–2*.
- Ondréas, H., Cannat, M., Fouquet, Y., Normand, A., Sarradin, P.M., and Sarrazin, J. (2009). Recent volcanic events and the distribution of hydrothermal venting at the Lucky Strike hydrothermal field, Mid-Atlantic Ridge. *Geochem. Geophys. Geosystems* *10*, Q02006.
- Perner, M., Hansen, M., Seifert, R., Strauss, H., Koschinsky, A., and Petersen, S. (2013). Linking geology, fluid chemistry, and microbial activity of basalt- and ultramafic-hosted deep-sea hydrothermal vent environments. *Geobiology* *11*, 340–355.
- Podowski, E., Ma, S., Luther, G., Wardrop, D., and Fisher, C. (2010). Biotic and abiotic factors affecting distributions of megafauna in diffuse flow on andesite and basalt along the Eastern Lau Spreading Center, Tonga. *Mar. Ecol. Prog. Ser.* *418*, 25–45.
- Podowski, E.L., Moore, T.S., Zelnio, K.A., Luther III, G.W., and Fisher, C.R. (2009). Distribution of diffuse flow megafauna in two sites on the Eastern Lau Spreading Center, Tonga. *Deep Sea Res. Part Oceanogr. Res. Pap.* *56*, 2041–2056.

- Portail, M., Olu, K., Escobar-Briones, E., Caprais, J.C., Menot, L., Waeles, M., Cruaud, P., Sarradin, P.M., Godfroy, A., and Sarrazin, J. (2015). Comparative study of vent and seep macrofaunal communities in the Guaymas Basin. *Biogeosciences Discuss.* *12*, 8497–8571.
- R Core Team (2015). *R: A Language and Environment for Statistical Computing* (Vienna, Austria: R Foundation for Statistical Computing).
- Ricciardi, A., and Bourget, E. (1998). Weight-to-weight conversion factors for marine benthic macroinvertebrates. *Mar. Ecol. Prog. Ser.* *163*, 245–251.
- Riou, V., Colaço, A., Bouillon, S., Khripounoff, A., Dando, P., Mangion, P., Chevalier, E., Korntheuer, M., Connelly, D., Serrao Santos, R., et al. (2010). Mixotrophy in the deep sea: a dual endosymbiotic hydrothermal mytilid assimilates dissolved and particulate organic matter. *Mar. Ecol. Prog. Ser.* *405*, 187–201.
- Sancho, G., Fisher, C.R., Mills, S., Micheli, F., Johnson, G.A., Lenihan, H.S., Peterson, C.H., and Mullineaux, L.S. (2005). Selective predation by the zoarcid fish *Thermarces cerberus* at hydrothermal vents. *Deep Sea Res. Part Oceanogr. Res. Pap.* *52*, 837–844.
- Sarradin, P.-M., Caprais, J.-C., Riso, R., Comtet, T., and Aminot, A. (1998). Brief account of the chemical environment at hydrothermal vent mussel beds on the MAR. *Cah. Biol. Mar.* *39*, 253–254.
- Sarrazin, J., and Juniper, S.K. (1999). Biological characteristics of a hydrothermal edifice mosaic community. *Mar. Ecol. Prog. Ser.* *185*, 1–19.
- Sarrazin, J., Juniper, S.K., Massoth, G., and Legendre, P. (1999). Physical and chemical factors influencing species distributions on hydrothermal sulfide edifices of the Juan de Fuca Ridge, northeast Pacific. *Mar. Ecol. Prog. Ser.* *190*, 89–112.
- Sarrazin, J., Levesque, C., Juniper, S., and Tivey, M. (2002). Mosaic community dynamics on Juan de Fuca Ridge sulphide edifices: substratum, temperature and implications for trophic structure. *CBM - Cah. Biol. Mar.* *43*, 275–279.
- Sarrazin, J., Sarradin, P.-M., Allais, A.-G., and Momareto Cruise Participants, X. (2006). MoMARETO: a cruise dedicated to the spatio-temporal dynamics and the adaptations of hydrothermal vent fauna on the Mid-Atlantic Ridge. *InterRidge News* *15*, 24–33.
- Sarrazin, J., Cuvelier, D., Peton, L., Legendre, P., and Sarradin, P.M. (2014). High-resolution dynamics of a deep-sea hydrothermal mussel assemblage monitored by the EMSO-Açores MoMAR observatory. *Deep Sea Res. Part Oceanogr. Res. Pap.* *90*, 62–75.
- Sarrazin, J., Legendre, P., de Busserolles, F., Fabri, M.-C., Guilini, K., Ivanenko, V.N., Morineaux, M., Vanreusel, A., and Sarradin, P.-M. (2015). Biodiversity patterns, environmental drivers and indicator species on a high-temperature hydrothermal edifice, Mid-Atlantic Ridge. *Deep Sea Res. Part II Top. Stud. Oceanogr.* *121*, 177–192.
- Schoener, T.W. (1970). Nonsynchronous spatial overlap of lizards in patchy habitats. *Ecology* *40*, 408–418.
- Schöne, B.R., and Giere, O. (2005). Growth increments and stable isotope variation in shells of the deep-sea hydrothermal vent bivalve mollusk *Bathymodiolus brevior* from the North Fiji Basin, Pacific Ocean. *Deep Sea Res. Part Oceanogr. Res. Pap.* *52*, 1896–1910.

- Sen, A., Becker, E.L., Podowski, E.L., Wickes, L.N., Ma, S., Mullaugh, K.M., Hourdez, S., Luther, G.W., and Fisher, C.R. (2013). Distribution of mega fauna on sulfide edifices on the Eastern Lau Spreading Center and Valu Fa Ridge. *Deep Sea Res. Part Oceanogr. Res. Pap.* 72, 48–60.
- Sen, A., Podowski, E.L., Becker, E.L., Shearer, E.A., Gartman, A., Yücel, M., Hourdez, S., Luther, G.W., III, and Fisher, C.R. (2014). Community succession in hydrothermal vent habitats of the Eastern Lau Spreading Center and Valu Fa Ridge, Tonga. *Limnol. Oceanogr.* 59, 1510–1528.
- Shank, T.M., Fornari, D.J., Von Damm, K.L., Lilley, M.D., Haymon, R.M., and Lutz, R.A. (1998). Temporal and spatial patterns of biological community development at nascent deep-sea hydrothermal vents (9°50'N, East Pacific Rise). *Deep Sea Res. Part II Top. Stud. Oceanogr.* 45, 465–515.
- Shillito, B., Bris, N.L., Hourdez, S., Ravaux, J., Cottin, D., Caprais, J.-C., Jollivet, D., and Gaill, F. (2006). Temperature resistance studies on the deep-sea vent shrimp *Mirocaris fortunata*. *J. Exp. Biol.* 209, 945–955.
- Singh, S.C., Crawford, W.C., Carton, H., Seher, T., Combiér, V., Cannat, M., Pablo Canales, J., Düsünür, D., Escartin, J., and Miguel Miranda, J. (2006). Discovery of a magma chamber and faults beneath a Mid-Atlantic Ridge hydrothermal field. *Nature* 442, 1029–1032.
- Tada, Y., Fujikura, K., Oguri, K., Kitazato, H., and Tanabe, K. (2009). In situ fluorochrome calcein marking of deep-sea molluscs using a new growth chamber. *Aquat. Ecol.* 44, 217–222.
- Taylor, V.F., Jackson, B.P., Siegfried, M.R., Navratilova, J., Francesconi, K.A., Kirshtein, J., and Voytek, M. (2012). Arsenic speciation in food chains from mid-Atlantic hydrothermal vents. *Environ. Chem.* 9, 130–138.
- Tilman, D., Lehman, C.L., and Thomson, K.T. (1997). Plant diversity and ecosystem productivity: Theoretical considerations. *Proc. Natl. Acad. Sci.* 94, 1857–1861.
- Tsurumi, M., and Tunnicliffe, V. (2001). Characteristics of a hydrothermal vent assemblage on a volcanically active segment of Juan de Fuca Ridge, northeast Pacific. *Can. J. Fish. Aquat. Sci.* 58, 530–542.
- Tsurumi, M., de Graaf, R.C., and Tunnicliffe, V. (2003). Distributional and Biological Aspects of Copepods at Hydrothermal Vents on the Juan de Fuca Ridge, north-east Pacific ocean. *J. Mar. Biol. Assoc. U. K.* 83, 469–477.
- Urcuyo, I.A., Massoth, G.J., Julian, D., and Fisher, C.R. (2003). Habitat, growth and physiological ecology of a basaltic community of *Ridgeia piscesae* from the Juan de Fuca Ridge. *Deep Sea Res. Part Oceanogr. Res. Pap.* 50, 763–780.
- Van Dover, C.L., and Doerries, M. b. (2005). Community structure in mussel beds at Logatchev hydrothermal vents and a comparison of macrofaunal species richness on slow- and fast-spreading mid-ocean ridges. *Mar. Ecol.* 26, 110–120.
- Van Dover, C.L., Humphris, S.E., Fornari, D., Cavanaugh, C.M., Collier, R., Goffredi, S.K., Hashimoto, J., Lilley, M.D., Reysenbach, A.L., Shank, T.M., et al. (2001). Biogeography and Ecological Setting of Indian Ocean Hydrothermal Vents. *Science* 294, 818–823.
- Warwick, R.M., and Gee, J.M. (1984). Community structure of estuarine meiobenthos. *Mar. Ecol. Prog. Ser.* 18, 97–111.

Warwick, R.M., and Price, R. (1979). Ecological and metabolic studies on free-living nematodes from an estuarine mud-flat. *Estuar. Coast. Mar. Sci.* 9, 257–271.

Zekely, J., Van Dover, C.L., Nemeschkal, H.L., and Bright, M. (2006). Hydrothermal vent meiobenthos associated with mytilid mussel aggregations from the Mid-Atlantic Ridge and the East Pacific Rise. *Deep Sea Res. Part Oceanogr. Res. Pap.* 53, 1363–1378.

Zeppilli, D., Vanreusel, A., Pradillon, F., Fuchs, S., Mandon, P., James, T., and Sarrazin, J. (2015). Rapid colonisation by nematodes on organic and inorganic substrata deployed at the deep-sea Lucky Strike hydrothermal vent field (Mid-Atlantic Ridge). *Mar. Biodivers.* 45, 489–504.

Accepted manuscript

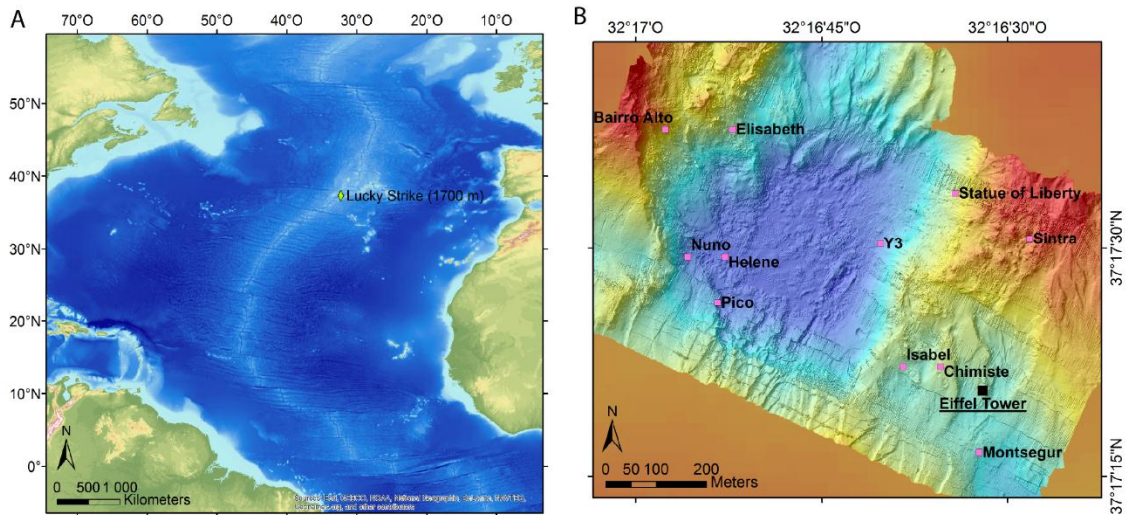


Figure 1. Map of the study site location. (A) Lucky Strike (LS) vent field on the Mid-Atlantic Ridge and (B) Eiffel Tower edifice in the geomorphological context of LS, with the central lava lake and surrounding active edifices (pink squares).

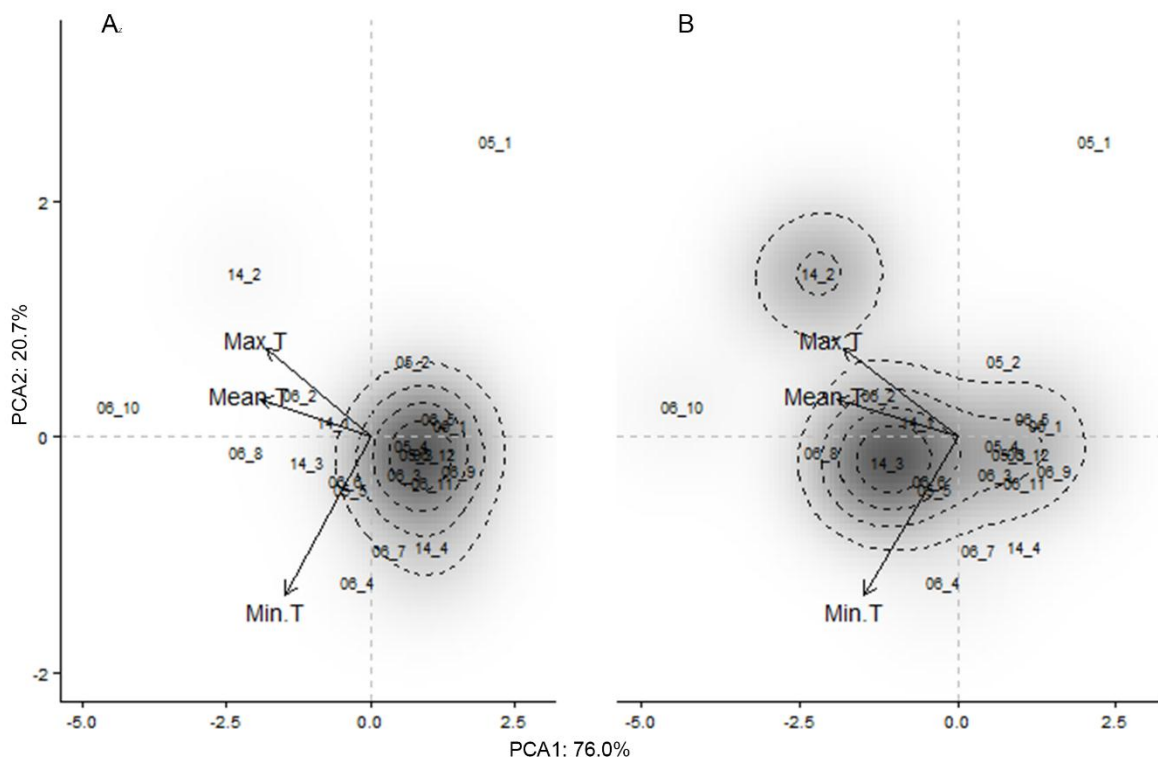


Figure 2. Thermal niche of *Bathymodiolus azoricus* in terms of density and dry weight. Grey gradient map of the 2D kernel density weighted by (A) squared relative densities or (B) dry weight of *B. azoricus* at each point of the gradient. Dashed contours indicate the levels of 80, 60, 40 and 20% of maximal kernel density, from the inner to the outer contours.

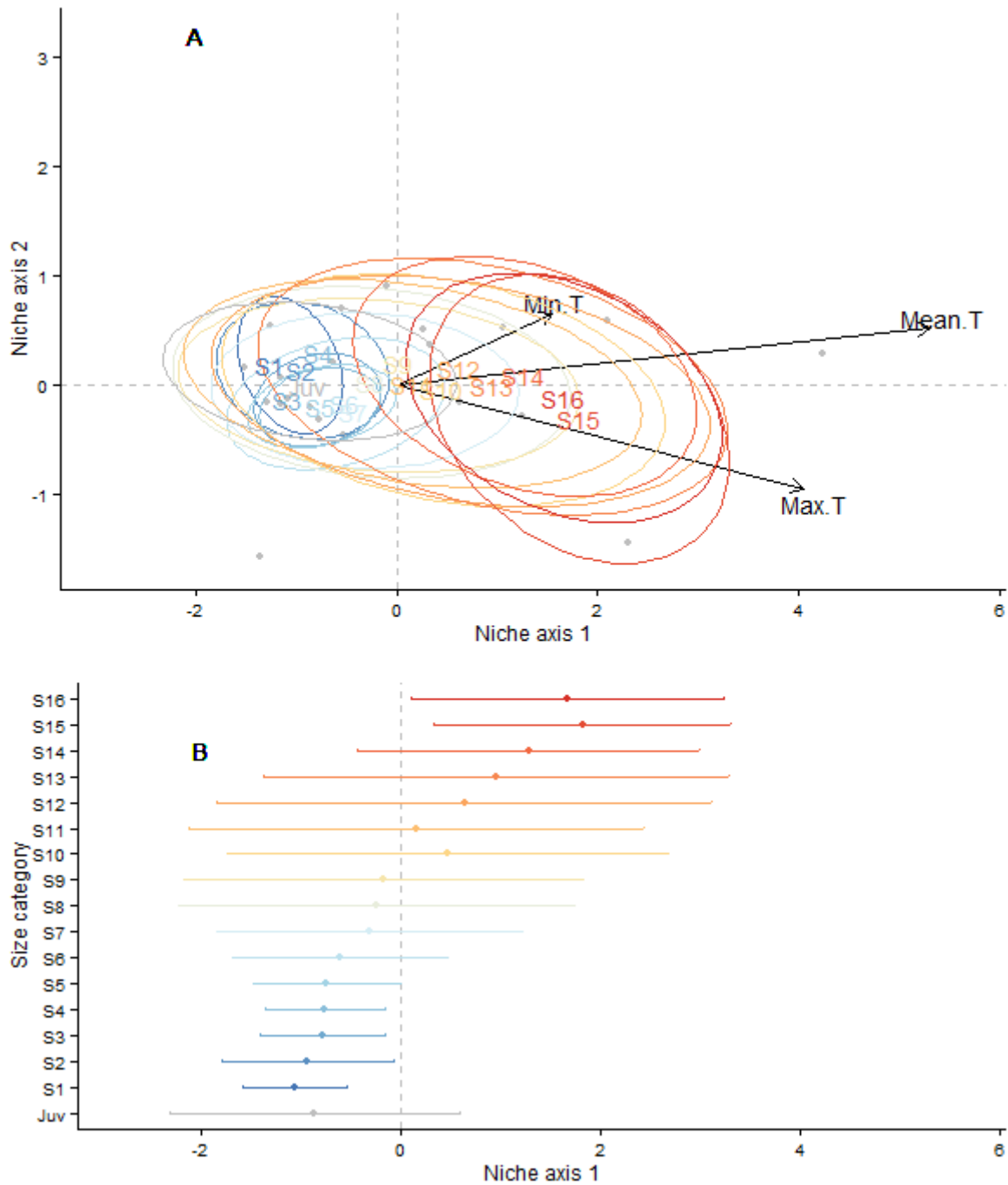


Figure 3. Thermal niches of mussel size categories. (A) OMI analysis two dimensional plot. Each ellipse represents the thermal niche of a size category. The centroid is the centre of gravity of samples weighted by the density of the size category. The ellipse is drawn as in the ade4 package, at a distance of $k \cdot \text{standard deviation}$, with $k=1.5$. The size category label is not always located at the center of the ellipsoid. (B) Mean position of size categories $\pm k$ standard deviation along the first axis of the niche analysis. Dotted line represents the second axis of the niche analysis.

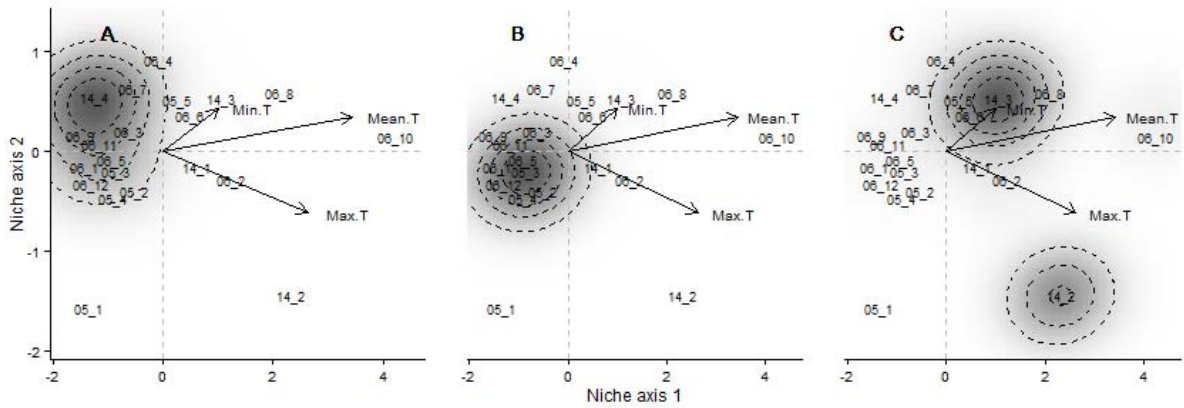


Figure 4. Thermal niches of three *Bathymodiolus azoricus* size clusters: (A) from size category S1 (5 mm) to S7 (35 mm), (B) from S8 (35 mm) to S14 (70 mm) and (C) greater than 70 mm. Grey areas map thermal conditions where the highest densities were observed. The arrows show the directions of the temperature variables in the new plot selected by the niche analysis to highlight differences in habitat selection.

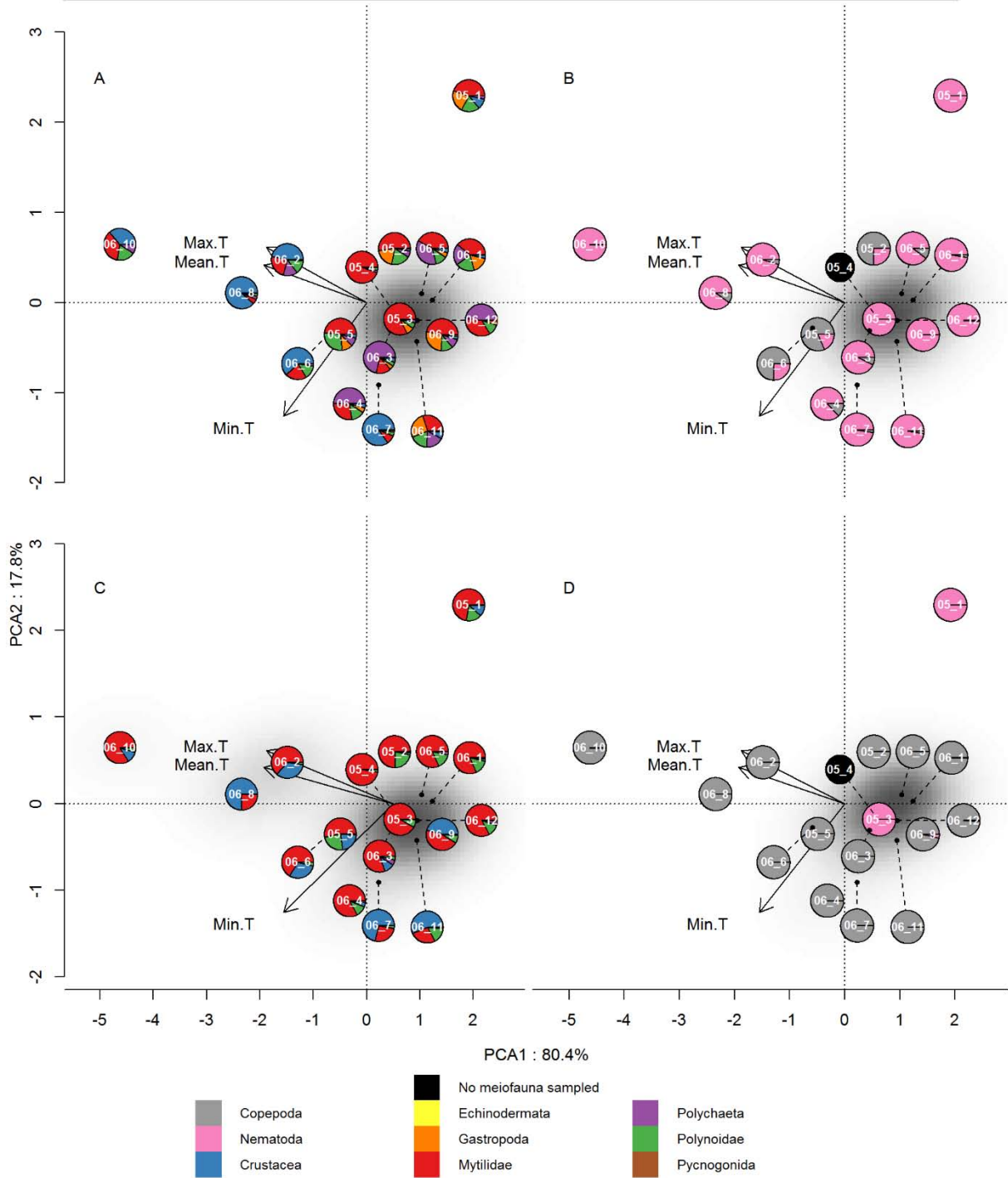


Figure 5. Relative proportion of taxa along the thermal gradient. (A) Macrofaunal abundance, (B) Meiofaunal abundance, (C) Macrofaunal dry weight, (D) Meiofaunal dry weight. Absence of meiofauna (plots B and D) in a sample is indicated in black.

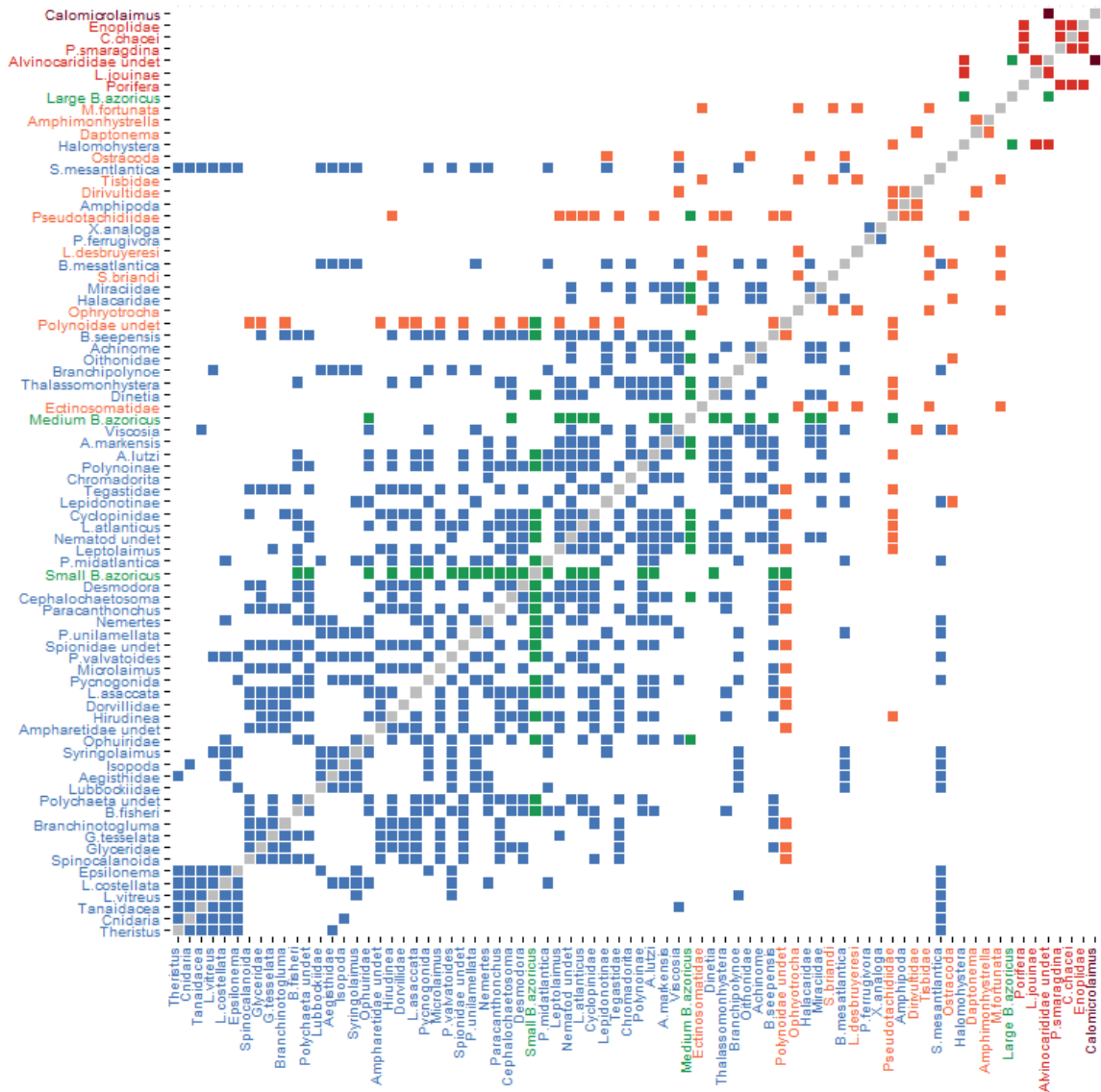


Figure 6. Niche similarities in the community. Row and column names are ordered according to their coordinates along the first axis of the niche analysis, from colder (*Theristus*) to hotter (*Calomicrolaimus*) coordinates. The colour code follows the results of the cluster analysis: brown for cluster 1 (Table 6), red for cluster 2 (Tables 6, 7a), orange for cluster 3 (Tables 6, 7b), which live in warmer habitats and blue for cluster 4 (Tables 6, 7c) in colder habitats. Green indicates niches that are similar to those of *Bathymodiolus azoricus* size classes. All squares shown in colour (not grey) indicate species pairs that have similar niches.

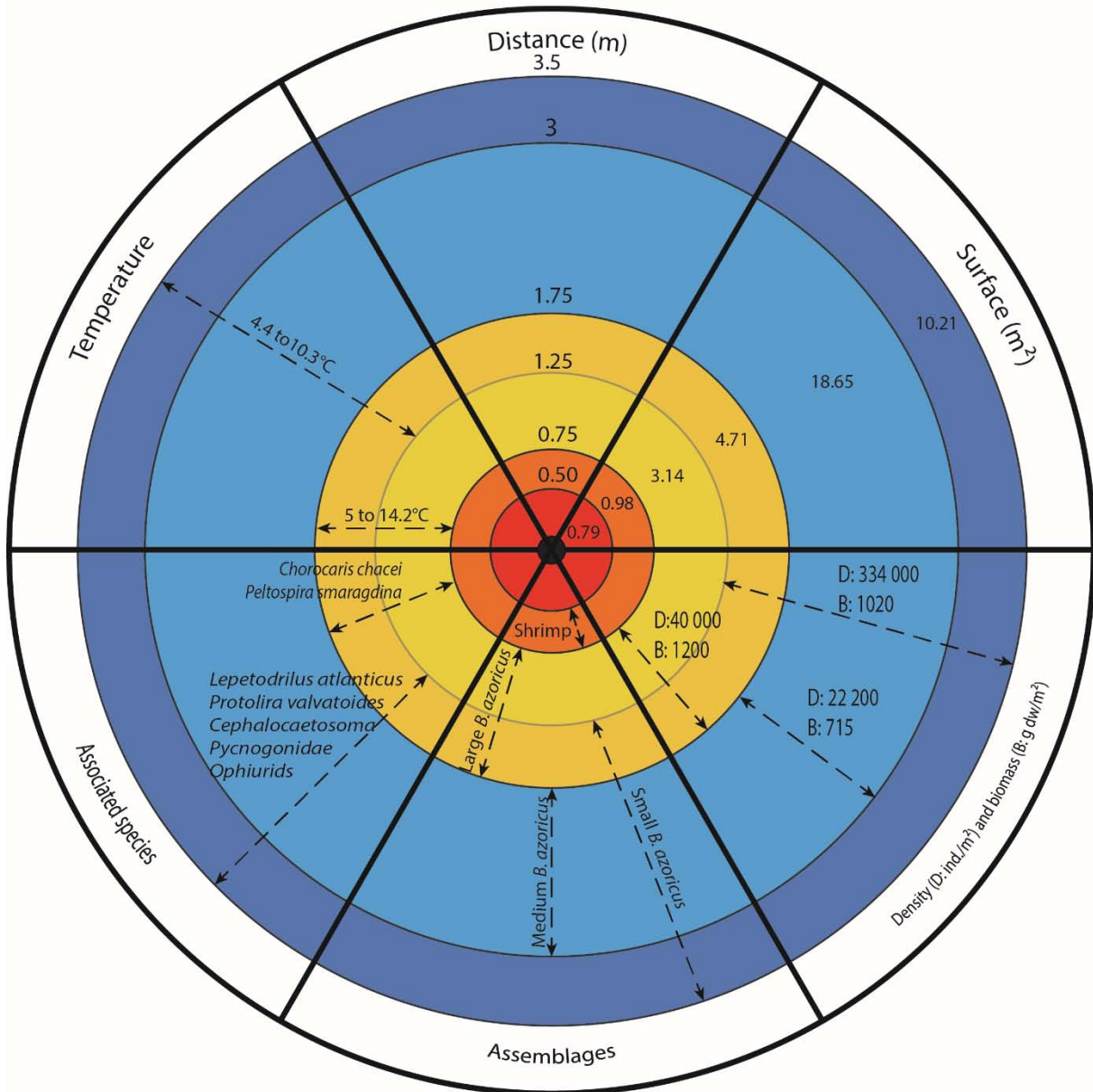


Figure 7. Diagram summarising the niche characteristics of mussel assemblages on the Eiffel Tower edifice. “Distance”: Distances D (m) to the black smoker from Cuvelier et al. (2009), “Surface” is available surface S (m²) calculated from $S=\pi D^2$, “Density and biomass”: densities and biomass associated with mussel assemblages along the gradient, “Assemblages” Mussel and shrimp assemblages distribution along the gradient, “Associated species”: Selection of abundant species associated with mussels, “Temperature”: Temperature ranges in the habitats where mussels live.

Supplementary figures

Figure S.1. Similarity test results on mussel size categories. Orange squares indicate when a pair of size categories has a similar niche.

Table 1. Sample collection and data used for analysis. (A) Mussel thermal ranges and (B) Mussel niche biotic descriptors (biomass and density of associated species). PCA, Principal component analysis; OMI, Outlier Mean Index; HC, Hierarchical clustering; SIM, niche similarity test.

		EXOMAR	MOMARETO	MoMARSAT 11	MoMARSAT 14
Cruise	Year	2005	2006	2011	2014
	Vessel	<i>L'Atalante</i>	<i>Pourquoi pas?</i>	<i>Pourquoi pas?</i>	<i>Pourquoi pas?</i>
	Remotely Operated Vehicle	<i>Victor6000</i>	<i>Victor6000</i>	<i>Victor6000</i>	<i>Victor6000</i>
Data	Type of experiment	Mussel assemblage sampling	Mussel assemblage sampling	Colonisation experiments	Mussel assemblage sampling
	Mussel beds sampled	5	12	0	4
	Fauna sampled	Meio and macrofauna	Meio and macrofauna	Meiofauna	Macrofauna
	Taxa inventory	41	71	0	0
	Taxa preservation	4% formalin, 70% ethanol after 2 days	4% formalin, 70% ethanol after 2 days	4% formalin	4% formalin
	Use	Species inventory	Species inventory	Biomass	Biomass
Data used for analysis of mussel niche	Mussel length and biomass	Yes	Yes	No	Yes
	PCA-, OMI-, HC- and SIM-mussel	Yes	Yes	No	Yes
Data used for analysis of community niches	Macrofaunal biomass	No	Yes	No	Yes
	Meiofaunal biomass	No	No	Yes	No
	PCA-, OMI-, HC- and SIM-community	Yes	Yes	No	No

Table 2. Mussel assemblages sampled during each cruise, with sampling surface (m²), total number of mussels sampled, total number of small (<5 mm) mussels, total density (ind./m²), and mean, minimal and maximal temperatures in the sampled assemblage.

Cruise	Mussel assemblages	Surface (m ²)	Total number of mussels	Small mussels (<5 mm)	Total density (ind./m ²)	Temperature (°C)		
						Mean	Min	Max
EXOMAR	05_1	0.040	29	0	725	5.3	3.7	6.7
	05_2	0.086	479	61	5570	5.48	4.4	7.4
	05_3	0.009	291	15	31630	4.95	4.6	7.0
	05_4	0.017	190	1	11176	4.95	4.6	7.4
	05_5	0.190	422	7	2221	6.08	4.8	7.4
MOMARET O	06_1	0.062	339	187	5468	4.91	4.4	5.8
	06_2	0.070	60	13	857	6.5	4.8	10.3
	06_3	0.082	183	90	2232	5.35	4.7	6.5
	06_4	0.049	185	72	3776	5.67	5.0	6.6
	06_5	0.049	395	208	8061	5.11	4.5	6.0
	06_6	0.077	61	13	792	6.04	4.8	7.8
	06_7	0.010	12	4	1200	5.39	4.8	6.1
	06_8	0.028	6	0	214	7.49	5.0	10.1
	06_9	0.013	94	53	7231	4.79	4.5	5.0
	06_10	0.061	90	32	1475	8.79	5.2	14.2
	06_11	0.033	163	102	4939	4.85	4.6	6.0
	06_12	0.032	281	124	8781	4.8	4.6	6.4
MoMARSAT 14	14_1	0.043	141	0	3310	6.09	4.7	9.2
	14_2	0.032	116	27	3659	6.81	4.7	14.1
	14_3	0.035	208	39	5926	6.74	4.8	8.5
	14_4	0.054	860	452	15985	4.84	4.7	5.2

Table 3. Length-weight relationships of three common taxa on Eiffel Tower edifice. W, weight (g); L, length (mm); n, number of individuals used to model the relationships.

	n	Flesh wet weight	R ²	Dry weight	R ²	Ash-free dry weight	R ²
<i>Bathymodiolus azoricus</i>	33	W=exp(-10.23)*L ^{2.93}	0.9	W=exp(-12.21)*L ^{2.93}	0.9	W=exp(-12.78)*L ^{3.02}	0.9
Polynoids	25	W=exp(-11.82)*L ^{3.60}	0.9	W=exp(-11.86)*L ^{3.06}	0.9	W=exp(-12.23)*L ^{3.15}	0.9
<i>Mirocaris fortunata</i>	90	W=exp(-13.35)*L ^{3.11}	0.9	W=exp(-10.23)*L ^{2.93}	0.9	W=exp(-10.23)*L ^{2.93}	0.9

Table 4. *Bathymodiolus azoricus* mussel size category limits (in mm) (Figure 3); mean and standard deviation of density (ind/m²); average mean, average minimal and average maximal temperatures (°C) in the habitat; absolute temperature minima

J u v	Size (mm)		Density (ind/m ²)		Average temperatures (°C)			Thermal range (°C)		OMI analysis				Permutati on test
	mi n	ma x	mea n	sd	mean	min	max	min	max	iner tia	o mi	tol	rto l	p.value
J u v	0	5	166 4	211 8	5.7	4.7	7.6	4.4	14.2	2.0 5	37 .7	46 .3	16 .0	0.0490*
S 1	5	10	367	779	5.3	4.6	6.7	3.7	10.3	1.6 6	70 .1	8. 6	21 .3	0.1420
S 2	10	15	351	658	5.5	4.6	7.2	3.7	14.2	1.5 9	57 .2	20 .7	22 .0	0.1595
S 3	15	20	676	184 0	5.6	4.6	7.4	3.7	14.2	0.9 9	65 .2	17 .6	17 .2	0.3956
S 4	20	25	899	238 3	5.6	4.6	7.6	3.7	14.2	0.9 6	65 .4	16 .8	17 .8	0.4174
S 5	25	30	667	149 2	5.7	4.6	7.8	3.7	14.2	1.0 3	57 .7	24 .5	17 .8	0.3421
S 6	30	35	306	464	5.5	4.6	7.3	3.7	14.1	1.3 6	30 .0	42 .5	27 .5	0.2527
S 7	35	40	201	202	5.4	4.6	7.2	4.4	14.1	1.5 3	7. 1	70 .1	22 .8	0.4657
S 8	40	45	186	183	5.8	4.6	7.7	3.7	14.2	2.4 6	2. 6	72 .9	24 .5	0.6277
S 9	45	50	133	134	5.8	4.7	7.9	4.4	14.2	2.2 6	1. 5	71 .0	27 .5	0.7927
S 10	50	55	119	144	5.9	4.7	8.1	3.7	14.2	3.1 1	7. 7	71 .5	20 .8	0.3028
S 11	55	60	97	96	5.9	4.7	8.0	4.4	14.2	2.9 2	1. 3	67 .2	31 .5	0.7800
S 12	60	65	78	90	5.9	4.7	8.1	4.4	14.2	3.8 1	11 .5	74 .1	14 .4	0.1078
S 13	65	70	59	87	6.0	4.7	8.4	4.4	14.2	4.1 5	23 .8	58 .8	17 .4	0.0561
S 14	70	75	46	85	6.3	4.8	9.0	4.4	14.2	3.6 0	47 .5	35 .6	16 .9	0.0584
S 15	75	80	43	89	6.7	4.8	9.9	4.4	14.2	5.2 9	65 .9	20 .9	13 .2	0.0109*
S 16	80	+	29	65	6.8	4.9	10.2	4.7	14.2	4.6 1	62 .5	25 .1	12 .4	0.0234*

and maxima in the habitat (°C); results of Outlier Mean Index analysis with inertia, marginality (OMI), tolerance (Tol), and residual tolerance (Rtol) as percentage of inertia and results of the permutation test (p.value). Asterisks indicate size classes with non-independent distribution regarding thermal variables.

Phylum	Class/sub-class	Order/Sub-Order	Family/Sub-family	Genus	species	C	N	weight (g)
Porifera	Unid.					2	2	n.a.
Cnidaria	Anthozoa	Actiniaria	Unid.			2	39	n.a.
				<i>Miractis</i>	<i>rimicarivora</i>	1	2	n.a.
	Alcyonaria					1	1	n.a.
Echinodermata	Ophiuroidea	Ophiurida	Ophiuridae	Unid.		2	3	2.90×10^{-02} ^[1]
Annelida	Polychaeta	Unid.				2	9	n.a.
		Amphinomida	Amphinomidae	<i>Archinome</i>	Unid.	2	2	n.a.
		Eunicida	Dorvilleidae	Unid.		2	32	n.a.
				<i>Ophryotrocha</i>	Unid.	2	318	2.00×10^{-04} ^[2]
		Phyllodocida	Glyceridae	Unid.		2	1	4.35×10^{-01} ^[1]
				<i>Glycera</i>	<i>tesselata</i>	2	2	
			Polynoidae	Unid.		2	157	2.80×10^{-01} ^[3] (259)
				<i>Branchinotogluma</i>	Unid.	2	6	
				<i>Branchinotogluma</i>	<i>fisheri</i>	2	2	
				<i>Branchinotogluma</i>	<i>mesatlantica</i>	2	12	
				<i>Branchipolynoe</i>	Unid.	2	72	
				<i>Branchipolynoe</i>	<i>seepensis</i>	3	959	
				<i>Lepidonotopodium</i>	<i>jouinae</i>	2	1	
			Polynoinae	Unid.		3	3	
			Lepidonotinae	Unid.		2	4	n.a.
		Spionida	Spionidae	Unid.		3	13	n.a.
				<i>Laonice</i>		2	5	n.a.
					<i>asaccata</i>			
				<i>Prionospio</i>		2	6	n.a.
					<i>unilamelata</i>			
		Terebellida	Ampharetidae	Unid.		3	1	n.a.
				<i>Amathys</i>	<i>lutzi</i>	2	199	2.20×10^{-02} ^[3] (45)
						4		
	Hirudinea	Unid.				2	2	n.a.
Mollusca	Bivalvia	Mytiloidea	Mytilidae	<i>Bathymodiolus</i>	<i>azoricus</i>	3	324	3.54 ^[3] (334)
						4		
	Caenogastropoda		Elachisiniidae	<i>Laeviphitus</i>	<i>desbruy</i>	3	6	n.a.

				<i>eresi</i>		
Vetigastro poda		Lepetodrilid ae	<i>Lepetodrilus</i> <i>atlanticus</i>	3	153	1.41×10^{-02} [3] (129)
			<i>Pseudorimula</i> <i>midatlantica</i>	3	70	5.74×10^{-03} [3] (59)
		Skeneidae	<i>Protolira</i> <i>valvatoides</i>	3	613	4.58×10^{-03} [3] (184)
Heterobran chia		Orbitestelli dae	<i>Lurifax</i> <i>vitreus</i>	3	10	n.a.
		Xylodisculi dae	<i>Xylodiscula</i> <i>analoga</i>	1	2	n.a.
Neomphali na		Pelstospirid ae	<i>Peltospira</i> <i>smaragdina</i>	2	2	n.a.
			<i>Lirapex</i> <i>costellata</i>	3	66	n.a.
Neritimorp ha		Phenocole padidae	<i>Shinkailepas</i> <i>briandi</i>	2	14	n.a.
Patellogas tropoda		Neolepetop sidae	<i>Paralepetop sis</i> <i>ferrugivora</i>	1	3	n.a.
Nemertea			<i>Nemertes</i> Unid.	2	20	n.a.
Arthropoda	Malacostraca	Amphipoda	Unid.	3	166	3.39×10^{-03} [3] (156)
		Isopoda	Unid.	2	1	n.a.
		Decapoda	Alvinocaridi dae	2	26	n.a.
			<i>Alvinocaris</i> <i>markensis</i>	1	4	n.a.
			<i>Mirocaris</i> <i>fortunata</i>	3	600	2.83×10^{-01} [3] (90)
			<i>Chorocaris</i> <i>chacei</i>	2	53	2.33 [3] (6)
		Bythograei dae	<i>Segonzacia</i> <i>mesantlantica</i>	3	22	1.40×10^{-01} [4]
		Tanaidacea	Unid.	3	22	8.07×10^{-03} [5]
Chelicerata	Pycnogonida	Unid.		2	21	n.a.
		Ammotheidae	<i>Sericosura</i> <i>heteroscela</i>	1	3	n.a.
Arachnida	Acari	Halacaridae	Unid.	3	79	n.a.
Ostracoda	Unid.			3	174	3.46×10^{-06} [3] (13)
Copepoda	Harpacticoida	Aegisthidae	Unid.	2	1	6.64×10^{-03} [3] (49)
		Ectinosomatidae	Unid.	2	3	n.a.
		Miraciidae	<i>Amphiascus</i>	3	525	6.64×10^{-03} [3] (49)
		Oithonidae	Unid.	2	1	5.22×10^{-03} [3] (8)

		Pseudotac hidiidae	Unid.		2	20	n.a.	
		Tegastidae	<i>Smacigaste s</i>	<i>micheli</i>	3	710 4	5.22×10^{-03} [3] (8)	
		Tisbidae	<i>Tisbe</i>	Unid.	3	57	8.08×10^{-03} [3] (20)	
	Cyclopoida	Cyclopinida e	<i>Heptnerina</i>	<i>confusa</i>	3	482	6.74×10^{-03} [3] (12)	
	Siphonosto matoida	Dirivultidae	<i>Aphotoponti us</i>	<i>atlanteu s</i>	3	264 0	6.74×10^{-03} [3] (12)	
			<i>Stygiopontiu s</i>	<i>rimivagu s</i>				
	Poecilosto matoida	Lubbockiida e	Unid.		2	1	n.a.	
	Spinocalan oida	Unid.			2	1	n.a.	
Nematod a	Unid.				2	696	n.a.	
	Chromado rea	Monhysteri da	Monhysteri dae	<i>Halomohyst era</i>	Unid.	2	140 78	2.30×10^{-07} [3] (14)
		Desmodori da	Draconema tidae	<i>Cephalocha etosoma</i>	Unid.	2	841 45	6.30×10^{-07} [3] (297)
			Draconema tidae	<i>Dinetia</i>	Unid.	1	97	5.00×10^{-07} [3] (12)
			Desmodori dae	<i>Desmodora</i>	Unid.	3	781 6	1.95×10^{-06} [3] (2)
			Microlaimid ae	<i>Microlaimus</i>	Unid.	2	113 86	4.20×10^{-07} [3] (16)
				<i>Calomicrolai mus</i>	Unid.	2	3	1.30×10^{-07} [3] (9)
			Epsilonem atidae	<i>Epsilonema</i>	Unid.	3	158	4.70×10^{-07} [3] (11)
	Plectida	Leptolamid ae	<i>Leptolaimus</i>	Unid.	3	179 46	n.a.	
	Chromador ida	Cyatholaini dae	<i>Paracantho nchus</i>	Unid.	3	339 0	1.60×10^{-06} [3] (3)	
		Chromador idae	<i>Chromadorit a</i>	Unid.	3	13	2.20×10^{-07} [3] (2)	
	Monhysteri da	Xyalidae	<i>Theristus</i>	Unid.	2	17	6.80×10^{-07} [3] (4)	
			<i>Daptonema</i>	Unid.	1	1	n.a.	
		Monhysteri dae	<i>Thalassomo nhystera</i>	Unid.	1	22	4.00×10^{-08} [3] (30)	
			<i>Amphimonh ystrella</i>	Unid.	1	1	n.a.	
	Enoplea	Enoplida	Ironidae	<i>Syringolaim us</i>	Unid.	3	481	n.a.
			Oncholaimi dae	<i>Viscosia</i>	Unid.	3	62	n.a.
		Enoploidea	<i>Enoplidae</i>	Unid.	2	17	n.a.	

Table 5. Taxa inventoried on the Eiffel Tower edifice. C, the cruise during which the taxa was sampled: 1: EXOMAR; 2: MOMARETO; 3: both cruises. N, the number of individuals found in the sampled assemblages. Mean wet individual weight (g) obtained from literature data: ¹ Kamenev et al. 1993, sublittoral hydrothermal vents, New Zealand; ² Bergquist et al. 2007, Endeavour, East Pacific Rise; ³ this study (number of individuals used); ⁴ Decelle et al. 2010, Logatchev, Mid-Atlantic Ridge; n.a., not available. Unid.: unidentified.

Table 6. Thermal tolerances of “rare” taxa (i.e. sampled only once), with observed density in the sample (ind./m²), cluster to which the taxa belongs, and mean, minimal and maximal temperatures at the sample site (Mean.T, Min.T and Max.T, in °C), unid: unidentified.

Taxon	Observed density (ind./m ²)	Cluster	Mean.T	Min.T	Max.T
Archinome	24	4	5.4	4.7	6.5
<i>Glycera tessellata</i>	32	4	4.9	4.4	5.8
Glyceridae	16	4	4.9	4.4	5.8
<i>Lepidonotopodium jouinae</i>	14	2	6.5	4.8	10.3
Ampharetidae unid.	20	4	5.1	4.5	6.0
Isopoda	30	4	4.9	4.6	6.0
<i>Alvinocaris markensis</i>	435	4	5.0	4.6	7.0
Amphimonhystrella	5	3	6.1	4.8	7.4
<i>Daptonema</i>	5	3	6.1	4.8	7.4
<i>Theristus</i>	1307	4	4.8	4.5	5.0
<i>Calomicrolaimus</i>	51	1	8.8	5.2	14.2
Enoplidae	42	2	7.5	5.0	10.1
Aegisthidae	30	4	4.9	4.6	6.0
Lubbockiidae	30	4	4.9	4.6	6.0
Oithonidae	12	4	5.4	4.7	6.5
Spinocalanoida	16	4	4.9	4.4	5.8

Table 7. Thermal tolerances of taxa from (a) cluster 2; (b) cluster 3; (c) cluster 4 (Figure 7). Number of samples (out of 17 samples) in which the species has been observed. Mean, maximum, and standard deviation (Sd) of densities are expressed as number of individuals per square meter. Optimal temperatures indicate thermal conditions at the site with maximum abundance. Limits indicate highest and lowest temperatures at which a species has been observed. Unid: unidentified.

Table 7 (a): Taxa	Sample	Density (ind/m ²)			Optimal temperatures			Limits (°C)	
		Max	Mean	Sd	Mean	Min	Max	Min	Max
Porifera	2/17	36	26	14	7.5	5.0	10.1	10.1	4.4
<i>Peltospira smaragdina</i>	2/17	36	25	16	7.5	5.0	10.1	10.1	4.8
<i>Chorocaris chacei</i>	6/17	821	211	322	7.5	5.0	10.1	14.2	4.7
Alvinocarididae unid.	6/17	148	74	47	8.8	5.2	14.2	14.2	4.6
Large <i>Bathymodilus azoricus</i>	13/17	443	200	140	8.8	5.2	14.2	14.2	4.4

Table 7 (b):

Ophryotrocha	5/17	3531	1290	1320	5.7	5.0	6.6	6.6	4.4
Polynoidea unid.	6/17	1551	563	667	5.1	4.5	6.0	7.8	4.4
<i>Laeviphitus desbruyeresi</i>	3/17	82	41	36	5.7	5.0	6.6	7.4	4.4
<i>Shinkailepas briandi</i>	4/17	1100	292	539	5.4	4.8	6.1	10.3	4.4
<i>Mirocaris fortunata</i>	14/17	10900	1423	2823	5.4	4.8	6.1	14.2	3.7
Ostracoda	12/17	727	273	232	4.9	4.6	6.0	14.2	4.4
Dirivultidae	14/17	8367	2682	3078	5.7	5.0	6.6	14.2	4.4
Ectinosomatidae	2/17	100	71	42	5.4	4.8	6.1	6.1	4.5
Pseudotachidiidae	5/17	102	68	33	5.7	5.0	6.6	10.3	4.4
Tisbidae	5/17	959	228	412	5.7	5.0	6.6	14.2	4.4

Table 7 (c):

Cnidaria	3/17	3000	1012	1722	4.8	4.5	5.0	7.4	4.4
Ophuridae	2/17	63	47	23	4.8	4.6	6.4	6.4	4.6
Dorvillidae	2/17	633	323	439	5.1	4.5	6.0	6.5	4.5
<i>Branchinotogluma</i> sp.	2/17	81	47	49	4.9	4.4	5.8	6.5	4.4
<i>Branchinotogluma fisheri</i>	2/17	31	24	11	4.8	4.6	6.4	6.4	4.4
<i>Branchinotogluma mesatlantica</i>	4/17	121	59	46	4.9	4.6	6.0	10.3	4.5
<i>Branchinotogluma seepensis</i>	17/17	2594	1052	905	4.8	4.6	6.4	14.2	3.7
<i>Branchipolynoe</i> sp.	3/17	1394	587	714	4.9	4.6	6.0	10.3	4.6
Polynoinae	3/17	31	16	13	4.8	4.6	6.4	7.4	4.4
Lepidonotinae	2/17	37	34	5	5.4	4.7	6.5	6.5	4.6
<i>Laonice asaccata</i>	4/17	41	25	13	5.1	4.5	6.0	6.5	4.4
<i>Pronospio unilamellata</i>	4/17	61	33	20	4.9	4.6	6.0	6.5	4.4
Spionidae unid.	4/17	143	71	73	5.1	4.5	6.0	7.4	4.5
<i>Amathys lutzi</i>	17/17	11594	2283	3422	4.8	4.6	6.4	14.2	3.7
Polychaeta unid.	3/17	94	62	44	4.8	4.6	6.4	6.5	4.4
Hirudinea	2/17	31	26	8	4.8	4.6	6.4	6.4	4.5
<i>Lepetodrilus atlanticus</i>	11/17	710	312	230	4.9	4.4	5.8	10.3	4.4
<i>Lurifrax vitreus</i>	4/17	385	114	181	4.8	4.5	5.0	7.4	4.4
<i>Pseudorimula midatlantica</i>	14/17	455	111	119	4.9	4.6	6.0	10.1	3.7
<i>Lirapex costellata</i>	8/17	1615	287	539	4.8	4.5	5.0	7.4	3.7
<i>Protolira valvatoides</i>	12/17	3923	1288	1355	4.8	4.5	5.0	10.3	3.7
<i>Xylodiscula analoga</i>	2/17	12	9	5	5.5	4.4	7.4	7.4	4.4
<i>Paralepetopsis ferrugivora</i>	2/17	23	14	13	5.5	4.4	7.4	7.4	4.4
Nemertes	4/17	182	107	68	4.9	4.6	6.0	6.5	4.5
Amphipoda	12/17	857	252	278	6.0	4.8	7.8	14.2	4.4
<i>Segonzacia mesatlantica</i>	7/17	154	79	60	4.8	4.5	5.0	10.3	4.5
Pycnogonida	9/17	231	87	84	4.8	4.5	5.0	7.4	4.4
Halacaridae	5/17	500	166	192	5.4	4.7	6.5	7.4	4.4

Tanaidacea	6/17	1077	206	427	4.8	4.5	5.0	7.4	4.4
<i>Halomohystera</i>	12/17	84317	21983	22434	6.5	4.8	10.3	14.2	4.4
<i>Thalassomonhystera</i>	4/17	326	127	138	5.0	4.6	7.0	7.4	3.7
<i>Cephalochaetosoma</i>	11/17	455170	149177	162639	4.8	4.6	6.4	14.2	4.4
<i>Leptolaimus</i>	12/17	142184	24502	50540	5.1	4.5	6.0	14.2	3.7
<i>Paracanthochus</i>	12/17	25852	5336	7683	5.1	4.5	6.0	14.2	4.4
<i>Desmodora</i>	10/17	71092	14001	24529	5.1	4.5	6.0	14.2	4.4
<i>Dinetia</i>	4/17	3043	884	1443	5.0	4.6	7.0	7.4	3.7
<i>Microlaimus</i>	15/17	126027	16662	33590	5.1	4.5	6.0	14.2	3.7
<i>Chromadorita</i>	10/17	64831	13407	20671	5.4	4.7	6.5	14.2	3.7
<i>Epsilonema</i>	4/17	3137	1141	1350	4.8	4.5	5.0	7.4	3.7
<i>Syringolaimus</i>	5/17	9304	2573	3998	4.9	4.6	6.0	7.4	3.7
<i>Viscosia</i>	5/17	261	157	95	4.8	4.5	5.0	7.4	3.7
Nematod unid.	5/17	5317	2300	2110	5.4	4.7	6.5	6.5	4.4
Cyclopinidae	8/17	3510	1042	1355	5.1	4.5	6.0	7.4	4.4
Miraciidae	9/17	3866	844	1211	5.4	4.7	6.5	10.3	4.4
Tegastidae	11/17	56347	10456	18144	5.1	4.5	6.0	10.3	4.4
Medium <i>Bathymodilus azoricus</i>	16/17	27717	3794	6885	5.0	4.6	7.0	14.2	3.7
Small <i>Bathymodilus azoricus</i>	16/17	5143	2085	1932	5.1	4.5	6.0	14.2	3.7